arXiv:1301.4470v3 [hep-ph] 25 Feb 2013

High Multiplicity pp and pA Collisions: Hydrodynamics at its Edge and Stringy Black Hole

Edward Shuryak and Ismail Zahed

Department of Physics and Astronomy,
Stony Brook University,
Stony Brook, NY 11794, USA

(Dated: February 26, 2013)

High Multiplicity pp and pA Collisions are a place where the macroscopic description (thermodynamics and hydrodynamics) meets with the microscopic one (pomerons and QCD strings). In the first part of the paper we study what happens with the hydrodynamical predictions as the system size gets smaller and smaller. For simplicity, we don't do it numerically, but analytically using Gubser$'$ s flow. We found that the radial flow is expected to increase, while the elliptic flow decreases, and high harmonics become perhaps too small to be observed. In the second part of the paper we approach the problem from the opposite side, using a string-based Pomeron model. We found that as the intrinsic temperature of the string grows, it approaches the Hagedorn regime and produces a high entropy string ball, amusingly dual to a certain black hole. Furthermore, when the string temperature narrows on the Hagedorn temperature or $T/T_H - 1 = \mathcal{O}(1/N_c)$, the stringy ball becomes a sQGP ball with non-negligible pressure and hydrodynamical flow.

I. INTRODUCTION

A. The outline

High energy heavy ion collisions are theoretically treated very differently from pp and pA ones. While the former are very well described using macroscopic theories – thermodynamics and relativistic hydrodynamics – the latter are subject to what we would like to call the "pomeron physics", described with a help of microscopic dynamics in terms of (ladders of) perturbative gluons, classical random gauge fields, or strings. The temperature and entropy play a central role in the former case, and are not even mentioned or defined in the latter case.

The subject of this paper is the situation when these two distinct worlds (perhaps) meet. In short, the main statement of this paper is that specially triggered fluctuations of the pp and pA collisions of particular magnitude should be able to reach conditions in which the macroscopic description will also become possible. While triggered by experimental hints at LHC to be discussed below, this phenomenon has not yet been a subject of a systematic study experimentally or theoretically, and is of course far from being understood. Needless to say, the problem touches on a number of key issues, we now enumerate and then address. From the macroscopic side, they are:

- What is the smallest system size which still undergoes a hydrodynamical explosion?
- How do all hydrodynamical observables scale with the system size R and viscosity-to-entropy ratio η/s, for such systems? In particular, how large are the viscous corrections for radial and elliptic flows?
- How do amplitudes of higher angular harmonics v_n scale with n,R and η/s? In which p_t region do we expect hydrodynamics to work, and for each v_n?
- Do high multiplicity pp and pA collisions in which the (double) "ridge" has been recently observed at LHC [7–9] fit into such a hydrodynamical scaling?

From the microscopic side we will use a stringy description of the pomeron at strong coupling in the context of holographic QCD with a confining wall. Specifically, we will use the recent model developed by Stoffers and Zahed [1, 2] where both the issue of a coherent scattering amplitude and entropy production can be adressed simultaneously. The issues we will address in this model are:

- What is the "intrinsic" string temperature, for the strings produced in the minimal-bias (unconstrained) pp and pA collisions? How does the multiplicity depend on the collision energy for the usual pomeron?
- What difference in the string shape and dynamics should be observed when the string becomes "near-critical" as its intrinsic temperature T approaches the Hagedorn temperature T_H?
- What are the energy, pressure, entropy and size of such a "near-critical" string?
- Is the thermodynamics of the near-critical string "holographic"? (Is it dual to a certain black hole?)
- If one uses the Kubo formula to evaluate the "string viscosity", what values are obtained ?
- For extremely strong fluctuations, with $T - T_H$ so small that the "string ball" thermodynamics changes from the Hagedron regime to the partonic (sQGP) one, what behavioral change is expected?

B. Phenomenology

The major objective of the heavy ion collision program is to create and study properties of a new form of matter, the Quark-Gluon Plasma. Among the many proposed signatures priginally in [3], a prominent place is taken by a collective "explosion", described by relativistic hydrodynamics. A major discovery at RHIC has been a robust radial and elliptic flow, in excellent agreement with hydrodynamics. This point is now also supported by LHC. The flow is characterized by higher angular moments $v_n(p_t)$ in the range of $p_t < 3\,GeV$, also in good agreement with hydrodynamical predictions.

One may naturally ask if large size colliding nuclei (AuAu at RHIC and PbPb at LHC) are really necessary for this description to hold, or if one can achieve this for smaller systems as well, such as those in pA or even pp collisions. In fact radial flow effects were searched for more than 30 years ago, in the minimum-bias pp collisions at CERN ISR [4], with negative results. Some weak indications for the radial flow have been found in specially triggered $\bar{\text{p}}$p collisions by the FERMILAB MINIMAX experiment [5], but the data remained inconclusive.

The "ridge" itself is an angular correlation in the azimuthal angle between two particles at $\Delta\phi < 1$ which extends to large rapidity range $|\Delta y| \geq 4$. Well known in AA collisions, it has been discovered by the CMS collaboration [6] in the first LHC run. In order to see it, one has to apply a very restrictive rare trigger. The CMS pp study had selected out of $\sim 10^9$ events only $\sim 10^3$, populating the highest multiplicity bin with a convincing ridge effect. More recently the same phenomenon was seen in pPb collisions as well, now by the CMS [7], ALICE [8] and ATLAS [9] collaborations. Larger number of "participant nucleons" and higher average multiplicity substantially weaken the requirements for the trigger: the "ridge" is seen at the trigger level of few percents higher multiplicity events. It is shown in those works that in pp and pA collisions, the same threshold in terms of multiplicity is needed to start showing the "ridge".

Angular correlations naturally appear as a consequence of a hydrodynamical explosion of a non-azimuthally symmetric objects. The spatial shape is then translated to momentum space and is observed. For example, in the comments on the CMS discovery written by one of us [10] it was illustrated by a string placed outside of an (axially symmetric) "stick of explosive. While the basic wind blowing is isotropic in ϕ, an extra string may move in a preferred direction. In central AA collisions it is similar to that. A symmetric explosion has perturbations in the form of localized "hot spots". But in general, any sufficiently deformed initial collisions for the fireball would be sufficient to create ridge-like correlations.

Furthermore, the subtraction of the so called "back-to back recoil" (a peak at $\phi \sim \pi$) which is either evaluated from some mini jet model (HIJING) or studied experimentally in the smaller multiplicity bins, reveals that a ridge is "doubled. The remaining correlation function is nearly symmetric with $\phi \approx 0$ and $\phi \approx \pi$ showing nearly the same correlation. In other words, there is a clearly dominance of the *second* angular harmonics [8, 9]. (This is unlike the central AA data, in which the strongest harmonics is the third $n = 3$.)

A number of authors described this phenomenon hydrodynamically. For the pA case, one may mention e.g. [11], which starts from Glauber-inspired initial conditions similarly to what is done in the AA case. Indeed, one proton propagating through the diameter of the Pb nucleus "wounds" 10-20 nucleons. Those are placed in certain random pattern in the transverse plane, providing some estimates of the higher angular harmonics ϵ_n from which hydrodynamical perturbations may start. The results are qualitatively consistent with the LHC data.

The objective of this paper is to extend such studies, using instead of a complicated "realistic models" with huge number of details and heavy numerics (the "event-by-event" hydrodynamics) an *analytic* approach. As we will see, this will allow us to focus on generic dependences of the predictions on the parameters of the problem.

C. Hydrodynamics

Before going to the details, let us express the main ideas and tools we have in mind in general terms. Since we will be discussing the validity of hydrodynamics, it is important to specify from the onset which hydrodynamics we will use.

The simplest are the equation of *ideal* hydrodynamics

$$\partial_\mu T^{\mu\nu} = 0 \tag{1}$$

containing the stress tensor in *local* approximation (no derivatives). Thus the only derivatives appear linearly and therefore simultaneous rescaling of the size and the evolution time $x^\mu \to \lambda x^\mu$ does not change the equation. So, ideal hydrodynamics will produce the same solution for fireball of any size, provided other parameters are unchanged. And indeed, such scaling was, for example, seen experimentally, e.g. for AuAu and CuCu collisions at RHIC. However, this works only if in *both* cases all viscous corrections are negligible.

At the very least, this requires as one applicability condition that the system's size R is much larger than some microscopic scales such as the inverse temperature T^{-1}. The corresponding ratio will be one small parameter which will subsequently change

$$\begin{aligned} \mathcal{O}(1) &\approx \frac{1}{TR^{pp,high\, mutiplicity}} \\ &> \frac{1}{TR^{central\, pA}} > \frac{1}{TR^{central\, AA}} \approx \mathcal{O}(1/10) \end{aligned} \tag{2}$$

Another important small parameter which we seem to have for strongly coupled Quark-Gluon Plasma (sQGP) is the *viscosity-to-entropy-density ratio*

$$\frac{\eta}{s} \approx \mathcal{O}(1/10) \ll 1 \tag{3}$$

Roughly speaking, it tells us that viscous effects – or the mean free path – is additionally suppressed compared to the micro scale $1/T$. The smallness of this second parameter suggests that one can hope to apply hydrodynamics even for systems as small as pp collisions, for which the former parameter is no longer small.

Hydrodynamical effects can be further separated into an overall explosion – called the *radial* flow, and higher angular harmonics of flow. The former is expected to be enhanced by larger gradients, while the latters get more suppressed by viscosity effects. Finally, one can discuss the applicability of hydrodynamics as a function of the particle transverse momentum $v_n(p_t)$.

We will show below that while in central AA we see about 6 angular harmonics, in pA only the second one remains relatively weakly damped by viscosity, while in the pp case even the second one is rather strongly damped. We still expect the radial flow (zeroth harmonics) to be enhanced, as the bulk viscosity is not supposed to be large enough in this case.

Furthermore, we will argue that the high multiplicity events in pp should be attributed to a QCD string going *near-critical*, with $T \to T_H$. If so, the transverse size $R_\perp^{pp}$ is of a sub-nucleon scale and is related to the significantly smaller QCD string scale

$$\sqrt{\alpha'} \approx (2\, GeV)^{-1} \approx 0.1\, \mathrm{fm} \tag{4}$$

D. Microscopic models

The usual (min-bias) pp and pA collisions are described by a number of models which use pomeron and reggeon exchange. Those terms originated from certain parameterization of the elastic and diffractive scattering amplitudes at high energy kinematics $\sqrt{s} \gg \sqrt{-t}$. The microscopic derivation in weak coupling is done via a (rapidity ordered) BFKL gluon ladders [12].

At strong coupling it is dominated by some form of a string (surface) exchange. In the AdS/CFT holographic context the discussion of elastic and inelastic amplitudes generated by such surface exchanges were originally addressed using bosonic variational surfaces [13, 14]. It has also been realized that the holographic pomeron can be associated with a spin-2 graviton exchange [15], in pure AdS with supersymmetry and conformal symmetry, which has triggered a rather extensive literature. In particular, a black-disk model [16].

Following on the semi-classical surface exchanges in [13, 14], a quantum bosonic string (surface) exchange model was suggested recently in Witten′ s confining background [17]. We will use its variant as discussed in [1, 2] in AdS$_5$ with a confining wall where the important number of transverse directions is physically identified. We will refer to this as the SZ model. Let us preview its physics in some general terms and detail it later.

One important idea is that the string which dominates semiclassically the scattering amplitude has some excitations, in the one-loop approximation. The quantum action helps to explain why the pomeron is supercritical and provides a specific assignment for its intercept $\alpha_{\mathbf{P}}(t=0)-1$. These excitations of the string modes can be described by a one parameter, an intrinsic (Unruh) temperature T. This temperature is set by the kinematics of the minimal bias collisions, but it can also fluctuate describing less usual events. When this temperature is small as compared to the so called Hagedorn temperature $T \ll T_H$, the string fluctuations are small and can be treated as a set of oscillators, as we schematically show in Fig.1a. This is the case for the traditional applications mentioned above, to the minimum-bias pp collisions at high energies up to LHC.

FIG. 1: String exchange between two sources (crosses) separated by the impact parameter **b**: the cold string case $\beta < \beta_H$ (a); the near-critical string case $\beta \to \beta_H$ (b).

With increasing collision energy the effective temperature grows and for some super-high collision energies (not reached at colliders) it may approach the Hagedorn temperature $T \to T_H$. At current energies (LHC) it can also happen, as fluctuations. We will argue that in this new regime the string will develop large excitations in the form of a *"string ball"* depicted in Fig.1b.

This near-Hagedorn regime is well known in finite-temperature QCD as the Polyakov-Susskind phenomenon and the coresponding entropy behavior is schematically shown in Fig.2. The entropy and energy asymptote infinity at $T \to T_H$ due to the proliferation of string states. The free energy and pressure remain finite. The rapid rise will be referred to as the "near-critical" or Hagedorn regime, also known as an interval with a "soft" equation of state

$$T \approx T_H, \; p \ll \epsilon \tag{5}$$

For a general review discussing effective strings and their role in the gluodynamics phase transition at finite and large N_c see e.g. [18].

Since in the prompt collision the pomerons override the reggeons at large $\sqrt{s}$, the collision is dominated by gluons instead of quarks. Therefore the pertinent Hagedorn regime is that of gluodynamics rather than QCD. We recall that the critical temperature in gluodynamics is $T_c^{YM} \approx 270$ MeV, which is significantly higher than the critical temperature in QCD which is $T_c^{QCD} \approx 165$ MeV. The former is important at the formation stage while the latter is important at freeze-out. In the effective string language, the transition in gluodynamics involves closed strings while that in QCD involves open strings. If we recall that the ratio of the closed to open string tensions is $\sigma_A/\sigma_F \approx 2$ and that the Hagedorn temperature is proportional to the square root of the string tension, we expect $T_c^{YM}/T_c^{QCD} \approx \sqrt{2}$, which is about the experimentally measured ratio.

We suggest that the behavior of a "string ball", created on a pomeron string as a fluctuation, near the Hagedorn temperature or $T \approx T_H$, should be very similar to that of strings in thermal equilibrium and close to deconfinement. The latter is referred to as the mixed phase of pure gauge theories with $N_c > 2$. Indeed, the gluodynamics transition is dominated by a dilute gas of close strings each of which carry a considerable stringy entropy. At the Hagedorn point, this stringy entropy is best packaged in a large and space filling string much like our string ball.

We further suggest that this Hagedorn phenomenon explains the significant increase of the produced entropy and thus multiplicity of secondaries. We believe its possible production in high-multiplicity pp collision is a new phenomenon not discussed previously. Another new element of our discussion (which is based on some recent ideas and technical progress in string theory) is the strong similarities we demonstrate between this "string ball" and the *black hole*, in terms of an effective temperature-entropy relations and even an effective viscosity we will evaluate.

Finally, we will argue that when the difference between T and T_H becomes very small and the energy (entropy) densities become as large as

$$\frac{\epsilon}{T_H^4} \approx \frac{s}{T_H^3} \approx N_c^2 \tag{6}$$

a second qualitative change happens: the "string ball" becomes explosive, as the pressure is no longer small. We argue by analogy with the thermodynamics of gauge theories: at some entropy density the mixed phase ends and the deconfined phase takes over. While we know it is so in equilibrium, we suggest the same should happen *out of equilibrium*, in a small fireball originating from a string ball in a Pomeron. Its direct observable consequence should be the appearance of a significant pressure $p \approx \epsilon/3$ and subsequent hydro explosion. The appearance of the (double) ridge in pp and pA collisions is perhaps the first observed experimental manifestation of this phenomenon.

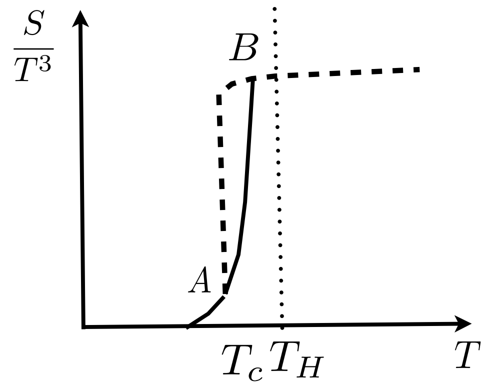

FIG. 2: Schematic temperature dependence of the entropy density. The dashed line represents equilibrium gluodynamics with a first order transition at $T = T_c$. The solid line between points A and B represents the expected behavior of a single string approaching its Hagedorn temperature T_H.

II. HYDRODYNAMICS AT ITS EDGE: STUDIES IN THE NAVIER-STOKES APPROXIMATION

A. Ideal radial flow using Gubser's solution

Many groups have studied heavy ion collisions by solving hydrodynamical equations numerically. However, it is not really necessary for the current purposes since there exist a relatively simple analytic solution found by Gubser [19], see also [20]. In this section we will apply this solution and compare the AA hydrodynamics with pA and pp ones.

Gubser flow is a solution which keeps the boost-invariance and the axial symmetry in the transverse plane. It is obtained via symmetry under special conformal transformation, and therefore, the matter is required to be conformal, with the EOS

$$\epsilon = 3p = T^4 f_* \tag{7}$$

where the parameter $f_* = 11$ is fitted to reproduce the lattice data on QGP thermodynamics.

The coordinates used are either the usual proper time -spatial rapidity - transverse radius - azimuthal angle set $(\bar{\tau}, \eta, \bar{r}, \phi)$ with the metric

$$ds^2 \;=\; -d\bar{\tau}^2 + \bar{\tau}^2 d\eta^2 + d\bar{r}^2 + \bar{r}^2 d\phi^2, \quad (8)$$

or the comoving coordinates we will introduce a bit later. The solution will depend only on the dimensionful variables $\bar{\tau}, \bar{r}$. The bar disappears because the solution has only one parameter q with dimension of the inverse length, so one can use rescaling to dimensionless variables

$$t = q\bar{\tau}, \;\; r = q\bar{r} \qquad (9)$$

Gubser's solution of ideal relativistic hydrodynamics, for the transverse velocity and the energy density reads

$$v_\perp(t,r) \;=\; \frac{2tr}{1+t^2+r^2} \qquad (10)$$

$$\frac{\epsilon}{q^4} \;=\; \frac{\hat{\epsilon}_0 2^{8/3}}{t^{4/3}\left[1+2(t^2+r^2)+(t^2-r^2)^2\right]^{4/3}}$$

where $\hat{\epsilon}_0$ is some normalization parameter.

The first task we perform is mapping the AA, pA and pp collisions to these coordinates, which is done via selection of the scale factors chosen as

$$q_{AA}^{-1} = 4.3, \;\; q_{pA}^{-1} = 1, \;\; q_{pp}^{-1} = 0.5\,(fm) \qquad (11)$$

and the energy density parameter, which is related to the entropy-per-rapidity density of the solution

$$\hat{\epsilon}_0 = f_*^{-1/3}\left(\frac{3}{16\pi}\frac{dS}{d\eta}\right)^{4/3} \qquad (12)$$

As in the Bjorken scaling solution, the rapidity interval is infinite and nothing depends on η, so the total entropy is infinite. Rapidity independence is well satisfied in the LHC data we discuss, in the observed rapidity interval. The entropy density is directly related to observed density of charged secondaries via a relation

$$\frac{dS}{d\eta} \approx 7.5\,\frac{dN_{ch}}{d\eta} \qquad (13)$$

defined at freezeout.

We use for central LHC AA=PbPb collisions

$$dN_{ch}^{AA}/d\eta = 1450 \qquad (14)$$

(Note that we ignore the difference between rapidity and pseudo rapidity.) The pp and pA data are split into several multiplicity bins: for definiteness, we will refer to one of them in the CMS set, with the (corrected average) multiplicity $N_{ch} = 114$ inside $|\eta| < 2.4$ and $p_t > 0.4\,GeV$ acceptance. We thus take

$$dN_{ch}^{pA}/d\eta = dN_{ch}^{pp}/d\eta = 1.6\,\frac{114}{2*2.4} \qquad (15)$$

where the factor 1.6 approximately corrects for the unobserved $p_t < 0.4\,GeV$ region.

Now the energy parameters are also fixed, and one can map the region in which hydrodynamics is supposed to work for all three collision regimes. Such a map is shown on the t, r plot in Fig.3. Hydrodynamics is assumed to be valid between the (horizontal) initial time lines and the contours of fixed freeze out temperature T_f. Note, that while the absolute sizes and multiplicity in central AA are quite different from pA, in the dimensionless variables those are closer to each other than in pp. The reason is an assumed factor of 2 jump in the radius.

Thus the cases get more and more "explosive", as the gradients progressively grow. The spectra should be calculated by the standard Cooper-Fry formula

$$\frac{dN}{d\eta dp_\perp^2} \sim \int p^\mu d\Sigma_\mu \,\exp\left(-\frac{p^\mu u_\mu}{T_f}\right) \qquad (16)$$

in which Σ_μ is the freeze out surface, on which the collective velocity $u_\mu(t,r)$ should be taken, for details see [24] . The transverse collective velocity on the freeze out curve is read off (10) which is too simple to plot. We just mention the maximal values reached at the "knee" of the freeze-out curves. They are

$$v_\perp^{max}[AA, pA, pp] = [0.69, 0.83, 0.95] \qquad (17)$$

respectively. For large p_t of the secondary a region around this "knee" dominates the integral. The slopes of the spectra of the relativistic pion are simply blue-shifted. Spectra of heavier particles – protons and antiprotons

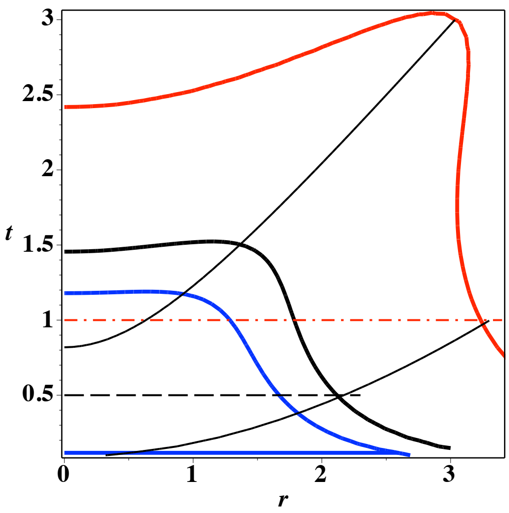

FIG. 3: (color online) The three horizontal lines correspond to the initial time: from bottom up AA (blue solid), pA (dash black) and pp (red dash-dot). The corresponding three curves with the same color are the lines at which the temperature reaches the same freeze-out value, set to be $T_f = 150\, MeV$. The two thin solid lines correspond to the values of the variable $\rho = -2.2$ (lower) and -0.2 (upper). Those values are used as initial and final values in the evolution of higher harmonics.

especially – are modified differently, leading to a strong enhancement of the proton/pion ratio at $p_t > 1 - 3\, GeV$. This effect, the manifestation of the collective radial flow, was suggested and searched for but not found in [4] using the min.bias ISR pp data long ago. It works spectacularly in AuAu collisions at RHIC and PbPb collisions at LHC. The same effect should be looked at in the (triggered) high multiplicity pA and pp events.

B. The viscosity effect on the radial flow

Here we continue to discuss the radial flow using Gubser's solution [19], now adding the viscosity effect. The equation for the reduced temperature $\hat{T} = \hat{\epsilon}^{1/4}$ using the combination of variables

$$g = \frac{1 - t^2 + r^2}{2t} \tag{18}$$

becomes an ordinary differential equation

$$3(1+g^2)^{3/2}\frac{d\hat{T}}{dg} + 2g\sqrt{1+g^2}\hat{T} + g^2 H_0 = 0 \tag{19}$$

where the last term contains a new prameter

$$H_0 = \frac{\eta}{\epsilon^{3/4}} = \frac{\eta}{s}\frac{4}{3}f_*^{1/4} \tag{20}$$

For $\eta/s = 0.134$ we will use as representative number $H_0 = 0.33$.

The equation is solvable analytically in terns of certain hypergeometric functions (see below) or numerically. For AA collisions we find that the role of the viscous corrections is truly negligible. The curves are the same within their plotted width. (This is, of course, well known from numerical studies in the literature during the last several years.) For the pA and pp cases one can see a difference between ideal and viscous , as we show in Figs. 4 through the reduced temperature dependence $T = \hat{T}/t$ at certain positions. The viscous effect is maximal at early times, and then the viscous and ideal curves meet. As expected, the viscous effects are very small at the fireball center $r = 0$, and become much more noticeable at its edge, see the $r = 3$ curve. In fact in this case the viscosity completely stops the cooling (decrease of the temperature) for a significant time, thus delaying the freezeout.

The main conclusion of this section is that a "realistic" viscosity of the sQGP is so small, that it provides a rather modest correction to the radial flow, even for the pA and pp collisions under consideration.

C. High angular harmonics

If the effects of order l/R are not negligible, they should be included. Keeping the first order gradient of the velocities leads to the celebrated Navier-Stokes hydrodynamics. As one includes the second order corrections, one get other known approximations such as the Israel-Stewart approximation. Recently, using the AdS/CFT approach about a dozen of lowest order coefficients in the gradient expansion were identified with alternating signs. An approximate PADE-like re-summation of these terms was suggested by Lublinsky and Shuryak [21].

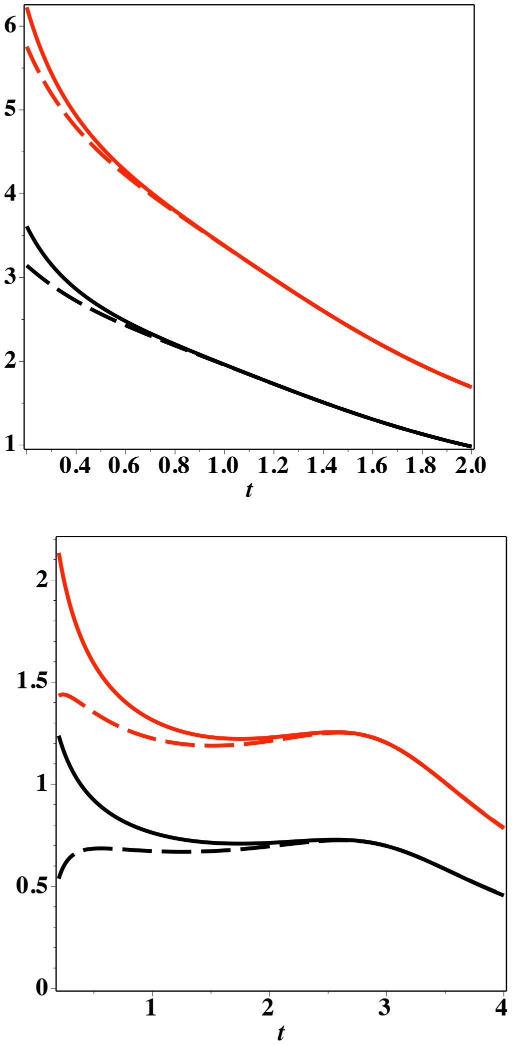

FIG. 4: (color online) The temperature versus dimensionless time t, for ideal hydrodynamics (solid) and viscous hydrodynamics with $\eta/s = 0.132$ (dashed) lines. The upper pair of (red) curves are for pp, the lower (black) ones for pA collisions. The upper plot is for $r = 1$, the lower plot for $r = 3$.

We will discuss the role of these higher order gradient corrections in section III.

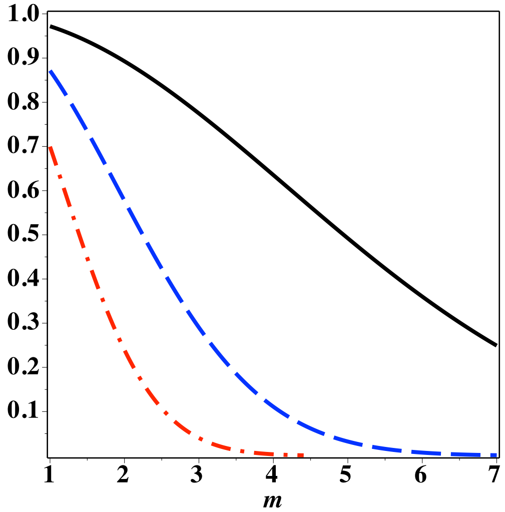

FIG. 5: (color online) Squared amplitude dissipation factor P_m^2 (as it appears in 2-particle correlators) for $\eta/s = .134$ as a function of the azimuthal harmonics m for AA (black) solid, pA (blue) dash and pp (red) dash-dot.

The effects of viscosity are likely to damp more the higher angular flow moments, as first discussed by Staig and Shuryak [22] and recenty applied to a wide range of RHIC data [23] . The "viscous filter" for the amplitude of a sound perturbation with the wave vector k is

$$P_k = \frac{\delta T_{\mu\nu}(t,k)}{\delta T_{\mu\nu}(0,k)} = \exp\left(-\frac{2}{3}\frac{\eta}{s}\frac{k^2 t}{T}\right) \qquad (21)$$

Since the scaling of the freeze out time is linear in R or $t_f \approx 2R$, and the wave vector k corresponds to the fireball circumference which is m times the wavelength, then

$$2\pi R = m\frac{2\pi}{k} \qquad (22)$$

Inserting these values in (21) yields

$$P_m = \exp\left[-m^2\frac{4}{3}\left(\frac{\eta}{s}\right)\left(\frac{1}{TR}\right)\right] \qquad (23)$$

The exponent contains the product of two small factors, η/s and $1/TR$ times the harmonics number squared. For PbPb LHC collisions one finds that

$$\frac{1}{TR} = \mathcal{O}(1/10) \qquad (24)$$

and a comparable η/s. For the most central bin – so that the elliptic flow does not obscure genuine higher harmonics via nonlinear effects – one can immediately see from this expression why we observed harmonics for $m = 1..6$, with $m \geq 7$ still in the statistical noise (see e.g. the comparison to hydrodynamics in [24]).

Proceeding to pp and pA collision (at LHC) by keeping a similar initial temperature $T_i \sim 400\,MeV \sim 1/(0.5\,fm)$ but a smaller size R, results in a macro-to-micro parameter that is no longer small, or $1/TR \sim 0.5, 1$, respectively. For a usual liquid/gas, with $\eta/s > 1$, there would not be any small parameter left and one would have to conclude that hydrodynamics is inapplicable for such a small system. However, since the quark-gluon plasma is an exceptionally good liquid with a very small η/s, which would keep this damping under control for $m = 0, 1, 2$, while harmonics with $m \geq 3$ would be hard to see.

D. Angular harmonics of Gubser flow

Unfortunately, the formulae we have used so far are, strictly speaking, only true for asymptotically high harmonics, with $m \gg 1$. Since we are actually interested in not so large $m = 2, 3$, we may check how the viscous filter works using a better approximation. For that, we return to Gubser's flow and consider its angular perturbations. The latters have been considered in the literature [20, 24].

In [20] Gubser and Yarom re-derived the radial solution by going into the co-moving frame via a coordinate transformation from the τ, r to a new set ρ, θ given by:

$$\sinh\rho = -\frac{1-\tau^2+r^2}{2\tau} \tag{25}$$

$$\tan\theta = \frac{2r}{1+\tau^2-r^2} \tag{26}$$

In the new coordinates the rescaled metric reads:

$$d\hat{s}^2 = -d\rho^2 + \cosh^2\rho\left(d\theta^2 + \sin^2\theta d\phi^2\right) + d\eta^2$$

and we will use ρ as the "new time" coordinate and θ as a new "space" coordinate. In the new coordinates the fluid is at rest, so the velocity field has only nonzero u_ρ. The temperature is now dependent only on the new time ρ. For nonzero viscosity the solution is

$$\hat{T} = \frac{\hat{T}_0}{(\cosh\rho)^{2/3}} + \frac{H_0\sinh^3\rho}{9(\cosh\rho)^{2/3}} \times {}_2F_1\left(\frac{3}{2}, \frac{7}{6}; \frac{5}{2}, -\sinh^2\rho\right) \tag{27}$$

with $\hat{T} = \tau f_*^{1/4} T$ and $f_* = \epsilon/T^4 = 11$ as in [19].

Small perturbations to Gubsers flow obey linearized equations which have also been derived in [20]. We start with the zero viscosity case, so that the background temperature (now to be called T_0) will be given by just the first term in (27). The perturbations over the previous solution are defined by

$$\hat{T} = \hat{T}_0(1+\delta) \tag{28}$$

$$u_\mu = u_{0\,\mu} + u_{1\mu} \tag{29}$$

with

$$\hat{u}_{0\,\mu} = (-1, 0, 0, 0) \tag{30}$$

$$\hat{u}_{1\mu} = (0, u_\theta(\rho,\theta,\phi), u_\phi(\rho,\theta,\phi), 0) \tag{31}$$

$$\delta = \delta(\rho,\theta,\phi) \tag{32}$$

The exact solution can be found by using the separation of variables $\delta(\rho,\theta,\phi) = R(\rho)\Theta(\theta)\Phi(\theta)$. In the non-viscous case, that we are now discussing, each of the three equations

$$R(\rho) + \frac{4}{3}\tanh\rho R(\rho) + \frac{\lambda}{3\cosh^2\rho}R(\rho) = 0$$

$$\Theta(\theta) + \frac{1}{\tan\theta}\Theta(\theta) + \left(\lambda - \frac{m^2}{\sin^2\theta}\right)\Theta(\theta) = 0$$

$$\Phi(\phi) + m^2\Phi(\phi) = 0 \tag{33}$$

are analytically solvable, with the results discussed in [24]. The parts of the solution depending on θ and ϕ can be combined in order to form spherical harmonics $Y_{lm}(\theta,\phi)$, such that $\delta(\rho,\theta,\phi) \propto R_l(\rho)Y_{lm}(\theta,\phi)$.

The basic equations for the ρ-dependent part of the perturbation, now with viscosity terms, can be written as a system of coupled first-order equations [20]. We are assuming rapidity independence, thus the system of equations (107),(108) and (109), from the referred paper, becomes two coupled equations, for (the

ρ-dependent part of) the temperature and velocity perturbations

$$\frac{d\vec{w}}{d\rho} = -\Gamma\vec{w}\ , \quad \vec{w}\ =\ \begin{pmatrix} \delta_v \\ v_v \end{pmatrix} \tag{34}$$

where the index v stands for viscous and the matrix components are,

$$\begin{aligned}
\Gamma_{11} &= \frac{H_0 \tanh^2\rho}{3\hat{T}_b} \\
\Gamma_{12} &= \frac{l(l+1)}{3\hat{T}_b \cosh^2\rho}\left(H_0 \tanh\rho - \hat{T}_b\right) \\
\Gamma_{21} &= \frac{2H_0 \tanh\rho}{H_0 \tanh\rho - 2\hat{T}_b} + 1 \\
\Gamma_{22} &= (8\hat{T}_b^2 \tanh\rho \\
&+ H_0\hat{T}_b\left(\frac{-4(3l(l+1)-10))}{\cosh^2\rho} - 16\right) \\
&+ 6H_0^2\tanh^3\rho)/(6\hat{T}_b\left(H_0\tanh\rho - 2\hat{T}_b\right))
\end{aligned} \tag{35}$$

Before we display the solutions, we need to translate our space-time plot into the $\rho-\theta$ coordinates. The initiation surface $t = t_i$ are *not* the $\rho = const$ surfaces. The freezeout ones also do not correspond to fixed ρ because the temperature is $T = \hat{T}(\rho)/t(\rho,\theta)$. So, in both cases one has to decide which points on the initiation and final surfaces are most important. The thin solid lines in Fig.3 approximately represent the initial ρ_i and the final ρ_f values for all three systems. Therefore, we will solve the equations between those two surfaces.

In Fig.6 we show the solution of the ρ evolution of the two variables, the temperature perturbation and velocity $\delta_l(\rho), v_l(\rho)$. As one can see, all of them start at $\rho_0 = -2$ from the same $\delta_l = 1$ value. While the elliptic one $l = 2$ (black solid curves) changes more slowly, higher harmonics oscillate more. The ratios v_m/ϵ_m are predicted by the hydrodynamical solution, complemented by the Cooper-Fry freezeout. Since the latter is rather involved (see [24] for discussion in detail) we will reason on the basis of the former alone. Assuming that the perturbation amplitudes are relatively small and everything scales approximately linear, and v_l at freeze out dominate, one can relate the relative magnitude of the harmonics into the measured two-particle correlation functions to scale as *squares* of the flow harmonics

$$\begin{aligned}
&(v_2^{AA})^2 : (v_2^{pA})^2 : (v_2^{pp})^2 \\
&= 0.5(\epsilon_2^{AA})^2 : 0.3(\epsilon_2^{pA})^2 : 0.16(\epsilon_2^{pp})^2
\end{aligned} \tag{36}$$

This is qualitatively consistent with the *squared* damping of the amplitude of the previous section, for $m = 2$.

A comparison to CMS data shows that the pp data show smaller v_2 as compared to pA data. Quantitatively, the ratio is about a factor of 1/4 (see Fig.3 of [7]) rather than 1/2 which the hydro solution provides. Perhaps it is because the pp collisions create a somewhat more spherical fireball, with $\epsilon_2^{pp} < \epsilon_2^{pA}$, in spite of having a smaller size. We will return to this issue at the end of the paper.

Let us now compare in a similar manner the ratio of the $m = 3$ to $m = 2$ harmonics

$$\begin{aligned}
\left(\frac{v_3^{AA}}{v_2^{AA}}\right)^2 &\approx 0.12\left(\frac{\epsilon_3^{AA}}{\epsilon_2^{AA}}\right)^2 \\
\left(\frac{v_3^{pA}}{v_2^{pA}}\right)^2 &\approx 0.09\left(\frac{\epsilon_3^{pA}}{\epsilon_2^{pA}}\right)^2 \\
\left(\frac{v_3^{pp}}{v_2^{pp}}\right)^2 &\approx 0.02\left(\frac{\epsilon_3^{pp}}{\epsilon_2^{pp}}\right)^2
\end{aligned} \tag{37}$$

Assuming $\epsilon_3/\epsilon_2 \sim 1$ one finds that in pA we predict $v_3/v_2 \approx 1/3$, which agrees nicely with the ALICE data [8]. For pp we have $v_3/v_2 \approx 1/7$ which is probably too small to be seen.

One may further ask why the experiment shows a very large $v_3/v_2 > 1$ in AA? The reason is explained in detail in [24]. It is related with the issue of the "sound horizon, and a larger temperature correction in the third harmonics in comparison to the elliptic term

$$\begin{aligned}
\left(\frac{\delta_3^{AA}(\rho_f)}{\delta_3^{AA}(\rho_0)}\right)^2 &\approx 1 \\
\left(\frac{\delta_2^{AA}(\rho_f)}{\delta_2^{AA}(\rho_0)}\right)^2 &\approx 0.1
\end{aligned} \tag{38}$$

which results into a very large contribution at freeze-out. This feature pointed out in [24] is nicely confirmed by the AA data (but not all hydro works). As one can see from our plots of $\delta_l(\rho)$, it is not the case for the pA and pp cases.

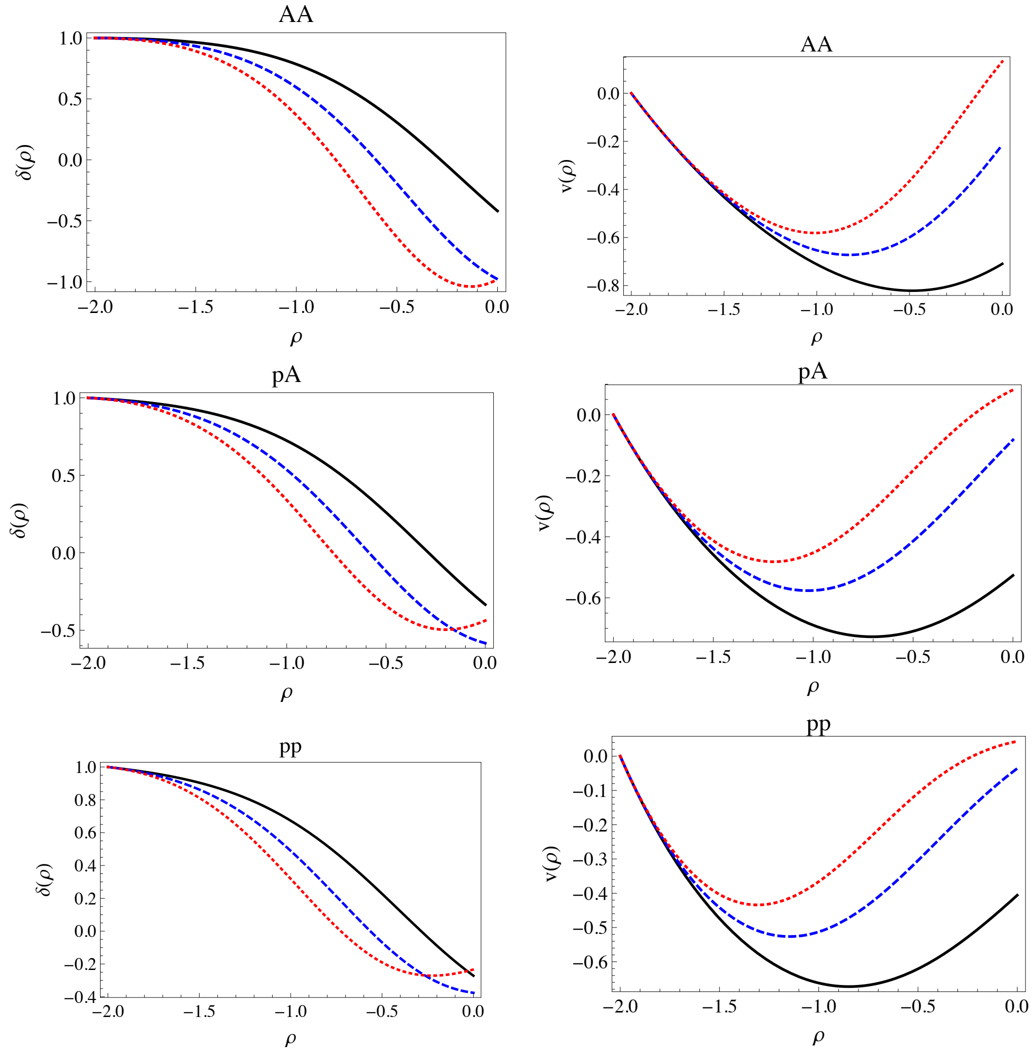

FIG. 6: (color online) The dimensional less temperature perturbation $\delta_l(\rho)$ and velocity $v_l(\rho)$, for $l = 2, 3, 4$ shown by (black) solid, (blue) dashed and (red) dotted curves, respectively. Three sets of calculations corresponds to AA, pA and pp collisions.

III. HIGHER GRADIENTS

A. The LS resummation

The Navier-Stokes approximation used so far only includes the first order terms in the gradient expansion. In this section we qualitatively discuss the role of the higher derivatives. Let us define symbolically the corresponding contribution to the stress tensor as

$$\delta T^{\mu\nu} = \sum_n c_n P_n^{\mu\nu}(T, u^\alpha) \sim \sum_n c_n \left(\frac{1}{TR}\right)^n \tag{39}$$

with coefficients c_n and certain kinematical structures with i derivatives $P_n^{\mu\nu}$. Their order of magnitude is given by the pertinent powers of the small hydro parameter $1/TR$. When these contributions are not small, they should be assessed, since they may cause the expansion to diverge.

AdS/CFT is an indispensable tool – in fact the only one we have – to address this issue for the sQGP. A consistent procedure deriving hydrodynamics and including in principle any number of gradients from Einsteins equation has been outlined in Ref. [26]. In practice, it has been worked out to second order only. However for small (linearized) perturbations the correlators of the two stress tensors can be calculated to higher order in frequency and wave vector ω, k, extending the original celebrated $\eta/s = 1/4\pi$ calculation [25] to about a dozen further coefficients.

An approximate PADE-like re-summation of the higher order terms has been suggested by Lublinsky and Shuryak (LS) [21]. The main point is to notice the alternating signs of the series, which calls for an re-summation a the geometrical series. Here we discuss only the single pole resummation model or LS2 in [21] in which the Navier-Stokes viscosity or NS is subtituted by an effective viscosity

$$\eta_{LS2}(\omega,k) = \frac{\eta_{NS}}{1-\eta_{2,0}k^2/(2\pi T)^2 - i\omega\eta_{0,1}/(2\pi T)} \tag{40}$$

Note that (40) involves only two dimensionless coefficients

$$\eta_{2,0} = -\frac{1}{2}\ \eta_{0,1} = 2 - \ln 2 = 1.30 \tag{41}$$

approximately reproducing all known terms as well as the large-k, ω behavior. The re-summation into the denominator suggests *reduced* viscous effect as k grows. As a result, the LS prediction is that in pp collisions one gets effectively a *smaller viscosity* than in AA!

This conclusion may sound too good to be true, and recently one of us has studied the "strong shock wave" problem [27] in the AdS/CFT setting, using first principles (solving Einstein equations) and comparing to the LS resummation scheme. While this problem is also "hydro-at-its-edge" type, the gradients of a shock profile have no small parameter $k/2\pi T \sim \mathcal{O}(1)$. The deviations between the NS and the exact (variational) solution of the corresponding Einstein equations were indeed found to be on the level of few percents only. Studies of time-dependent collisions in bulk AdS/CFT have found that the first-principle solution approaches the NS solution early on and quite accurately, at the time when the higher gradients by themselves are not small [28].

Changing k^2, ω into derivatives

$$\begin{aligned} -k^2/q^2 &\rightarrow (\frac{\partial}{\partial r})^2 + \frac{1}{r}\frac{\partial}{\partial r} \\ i\omega/q &\rightarrow \frac{\partial}{\partial t} \end{aligned} \tag{42}$$

makes the re-summed factor (with the denominator) an integral operator. For any function of the coordinates $f(t,r)$ we define the "LS operator" acting on a function f as

$$\begin{aligned} \mathbf{O}_{LS}^{-1}(f) = &\quad 1 + \frac{q^2}{2(2\pi T)^2}\left(\frac{\partial^2 f}{\partial r^2} + \frac{1}{r}\frac{\partial f}{\partial r}\right)\frac{1}{f} \\ &+ (2-\ln 2)\,\frac{q}{2\pi T}\frac{\partial f}{\partial t}\frac{1}{f} \end{aligned} \tag{43}$$

Schematically the resummed hydro equations look as

$$(Euler) = \eta\mathbf{O}_{LS}(Navier - Stokes) \tag{44}$$

where $\mathbf{O}_{LS}$ is an integral operator. However, one can act with its inverse on the hydrodynamical equation as a whole, acting on the Euler part but canceling it in the viscous term

$$\mathbf{O}_{LS}^{-1}(Euler) = \eta(Navier - Stokes) \tag{45}$$

These are the equations of the LS hydrodynamics. Obviously they have two extra derivatives and thus need more initial conditions for solution.

Instead of solving these equations, we will simply check the magnitude of the corrections appearing in the l.h.s due to the action by the LS differential operator on the (ideal Gubser) solution used as a zeroth-order starting point. As one can see, large systems have a small $q/T \sim 1/RT$ parameter and so these corrections are *parametrically* small. The issue is what happens "on the hydro edge", when the corrections have no formal small parameter.

In Fig.7 we show the (inverse) action of (43) on the zeroth other temperature profile of the Gubser flow as a function of r. We have used the freeze-out temperature $T_f = 150\,MeV$ and the indicated respective freeze-out times for pp, pA and AA. The higher gradient corrections for

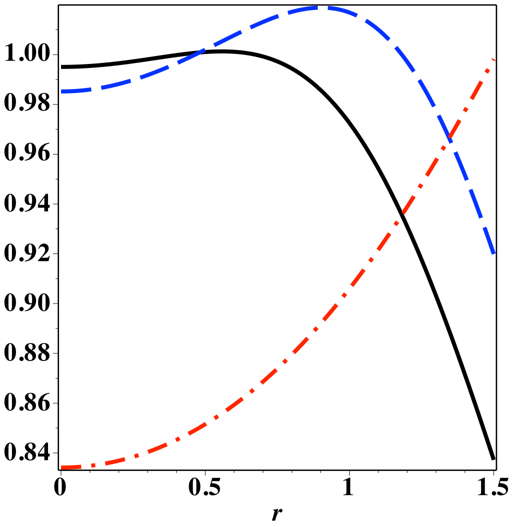

FIG. 7: (color online) The action of the LS operator O_{LS} (43) on the zeroth order (non-viscous) temperature profile, the first term of (27). The three lines correspond to AA (black) solid, pA (blue) dashed and pp (red) dash-dot.

AA and pA are inside the few percent range from 1, while in the pp case the correction is larger, yet still in the 15 percent range. We thus conclude, that if the LS resummation represents the role of the higher gradients, the overall corrections remain manageable even for the pp case.

B. The momentum dependence of the harmonics and viscosity at freeze out

The issue of higher gradients should also be addressed at the kinetic level, as emphasized by Teaney [29]. Equilibrium local distribution function of (quasi)particles should be corrected by the gradient expansion terms

$$f(p) = f_0(p) + f_1(p)\frac{\eta}{s}p^\mu p^\nu \partial_\mu u_\nu + (\text{higher gradients}) \quad (46)$$

which are negligible in the macroscopic limit $TR \to \infty$ but not in the "hydro-at-its-edge" problems like the pp case we discuss here. The main point in [29] is that Lorentz covariance forces any extra derivative to carry a particle momentum. As a result, the expansion parameter of the n-th term is

$$\frac{\eta}{s}\left(\frac{p}{T}\frac{1}{TR}\right)^n \quad (47)$$

In AA collisions the smallness of the second factor allows p/T to become large or $\mathcal{O}(10)$, before the macroscopic theory breaks down. Indeed, the higher harmonics of the flow agree with this estimate for transverse momenta of the order of $p_t \approx 3\,\text{GeV}$, or $p_t/T_f \approx 20$.

Following this line of reasoning, and turning to the case of pp and pA collisions, the second parameter is no longer small. Therefore we expect the validity region of the macroscopic theory to be strongly reduced, say to a much smaller region in $p_t/T_f \sim \mathcal{O}(1)$.

We know it cannot be correct, as both CMS and ATLAS are not even able to observe soft particles. In fact, as seen from Fig.4e of [9], the elliptic flow $v_2(p_t)$ in pA rises linearly to about 2 GeV/c, where the presummed viscosity effects cause it to start decreasing. Furthermore, the elliptic flow reaches there a magnitude comparable with that in AA collisions. So, apparently the experiment does not see an expected reduction of the hydro validity region!

The only way we think the data can be consistent with theory is because the viscosity η/s should not be treated as a universal constant. While its value extracted from hydro calculations of v_n is an average over the whole duration of the collision, the viscosity we discuss now is at freeze-out. Perhaps its effective value there is even smaller than the average.

IV. FROM THE USUAL TO EXPLOSIVE POMERON

A. The SZ model: classical strings and Polyakov tachyon contributions

The SZ model [1, 2] is based on bosonic string exchanges between the colliding high energy objects. It is essential that the QCD string with a nonzero tension related to QCD confinement is used, and *not* the conformal superstring which has a massless spin-2 graviton ex-

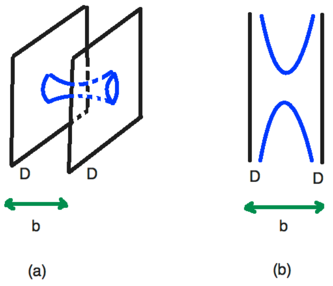

FIG. 8: Dipole-dipole scattering with separation $\mathbf{b}$: pomeron exchange (a); reggeon exchange (b).

citation. There is no supersymmetry and gravitons transmutes to a massive spin-2 glueball with an exponentially small contribution in the pomeron diffusive limit [14, 17]. However there is still a large N_c parameter, related with a small string coupling g_s and a large 't Hooft coupling $\lambda = g_s N_c$ so that $1/\lambda$ effects of the curved geometry will be considered as subleading.

At very high energies the rapidity interval parameter can be used as a large parameter

$$\chi = \ln(s/s_0) \gg 1 \tag{48}$$

It will play the role of the *effective time* in what follows. Transverse momentum transfer is held fixed $t = -q^2$ and soft. The main phenomenon to be studied is the string diffusion. Two longitudinal directions – time and the beam direction, also often used as light cone variables $x_\pm$ – are complemented by two transverse coordinates plus a *"scale coordinate"* z. Its initial value corresponds to a physical size of the colliding dipoles and diffusion means the production of small size closed strings. The z-coordinate is not flat. We will model its metric by an AdS$_5$ with a wall. The number of transverse coordinates, which will play an important role in the following, is thus

$$D_\perp = 3 \tag{49}$$

We will now review the pomeron results and its associated entropy in this setting. The amplitude of the elastic dipole-dipole scattering in Fig. 8a reads [1, 2, 17]

$$\frac{1}{-2is}\mathcal{T}(s,t;k) \approx g_s^2 \int d^2\mathbf{b}\, e^{iq\cdot\mathbf{b}}\, \mathbf{K}_T(\beta,\mathbf{b};k) \tag{50}$$

where $\mathbf{K}_T$ is the pomeron propagator for dipole sources of color N_c-ality k describing the string flux. k runs over all integers till $N_c/2$ for even N_c and $N_c/2 + 1/2$ for odd ones. In the real world with the SU(3) color group, $k = 1$ is the usual string between fundamental charges (quarks) and the largest tension $k = 2$ is the one between two baryon junctions. The first argument of the propagator is $\beta = 2\pi\mathbf{b}/\chi$, where $\mathbf{b}$ is the impact parameter. $g_s \approx 1/N_c$ is the string coupling.

The explicit form of $\mathbf{K}_T$ for the standard long strings regime

$$\mathbf{b} > \beta > \beta_H \tag{51}$$

follows from the Polyakov string action,

$$\mathbf{K}_T(\beta,\mathbf{b};k) = \left(\frac{\beta}{4\pi^2\mathbf{b}}\right)^{D_\perp/2} \times \sum_{n=0}^{\infty} d(n)\, e^{-\sigma\beta\mathbf{b}\left(1-\beta_H^2/2\beta^2+4\pi n/\sigma\beta^2\right)} \tag{52}$$

We have defined $\sigma = \sigma_T/2$, the Hagedorn inverse temperature as

$$\beta_H = \sqrt{\pi D_\perp/3\sigma} \tag{53}$$

and the inverse temperature as

$$\beta_U = \beta/k = \frac{2\pi\mathbf{b}}{\chi k} \tag{54}$$

The subscript U is a reminder that it is basically the Unruh temperature related to a fixed acceleration/tension. The asymptotic string density of states is

$$d(n) \approx e^{2\pi\sqrt{D_\perp n/6}}/n^{D_\perp/4} \tag{55}$$

with the normalization $d(0) = 1$.

For high energies and large $\mathbf{b}$ – long strings – the pomeron propagator $\mathbf{K}_T$ to leading order in $1/\lambda$ obeys a diffusion equation in rapidity χ and curved transverse space

$$\left(\partial_\chi + \mathbf{D}_k\left(\mathbf{M}_0^2 - \nabla_\mathbf{b}^2\right)\right)\mathbf{K}_T = 0 \tag{56}$$

with $\mathbf{D}_k = \alpha'/k = l_s^2/k$ the pomeron diffusion constant. This diffusion (56) is reminiscent of Gribov diffusion and implies on average $\langle b^2 \rangle = \mathbf{D}_k \chi$ for close pomeron strings. For large $\mathbf{b}$ and confining AdS backgrounds, the diffusion takes place near flat geometry (BH horizon or wall) with a tachyon mass related to string modes

$$\mathbf{M}_0^2 = \frac{4D_\perp}{\alpha'} \left(\sum_{n=1}^{\infty} \frac{n}{e^{2\chi n/k} - 1} - \frac{1}{24} \right) \qquad (57)$$

with $D_\perp = 3$ in AdS$_5$ with a wall. While we describe quantum string dynamics at zero temperature, the formulae resemble thermodynamical ones. This happens because the string-membrane configuration in question, depicted in Fig.8(a) is a tube, and quantization on a circle is formally identical to thermal Matsubara-time formalism.

The extra z coordinate is different from others. A finite size dipole sitting at a height z a finite distance from the confining wall, experiences corrections $O(\lambda^{-1/2})$ due to the curvature in z. This results in a shift of the tachyon mass

$$\mathbf{M}_0^2 \to \mathbf{M}_0^2 + \frac{(D_\perp - 1)^2}{4\alpha' \sqrt{\lambda}} \ . \qquad (58)$$

Most of the arguments to follow will be carried out for large $\lambda \gg 1$ unless indicated otherwise, so this effect is considered small.

Inserting the leading $n = 0$ contribution of (52) in (50) yields the pomeron contribution to the elastic dipole-dipole scattering amplitude at large χ and fixed N-ality k

$$\mathcal{T}(s, t; k) \approx i g_s^2 \left(\frac{s}{s_0} \right)^{1 + \frac{kD_\perp}{12} + \frac{\alpha'}{2k} t} \qquad (59)$$

Thus the resulting pomeron has the intercept above 1 (and corresponds to cross section growing with energy)

$$\alpha_{\mathbf{P},k}(0) = 1 + \frac{kD_\perp}{12} \to 1 + \frac{kD_\perp}{12} - \frac{(D_\perp - 1)^2}{8\sqrt{\lambda}} \qquad (60)$$

where the first term is due to Casimir-Luscher contribution and the $1/\sqrt{\lambda}$ correction follows from the tachyonic correction (58) as discussed in [1].

The subcritical string regime discussed so far is defined by the condition $\beta = 2\pi \mathbf{b}/\chi > \beta_H$ which translates to a rapidity range (collision energies) $\chi < 2$ in the diffusive limit $\langle b^2 \rangle = D_k \chi$. A more precise bound follows from the inclusion of the $1/\lambda$ corrections in the tachyon mass (58) or

$$\beta > \sqrt{2(\alpha_{\mathbf{P}} - 1)}\, \beta_H \qquad (61)$$

This leads to the bound $\chi < 10$ for the corrected phenomenological value of the pomeron intercept $\alpha_{\mathbf{P}} - 1 = 0.08$ in (60), which roughly corresponds to energies below the LHC. This condition discriminates between a sub-critical and a critical string as we will detail below. We note that (61) implies a strong coupling renormalization of the Hagedorn temperature through the geometry of AdS.

B. Reggeon

For completeness, we note that reggeon exchange with open strings can be addressed similarly. For the Reggeon $\sigma = \sigma_T$ and the elastic scattering amplitude for dipoles of N-ality k as shown in Fig. 8 b is now

$$\mathcal{T}(s, t; k) \approx i g_s^2 \left(\frac{s_0}{s} \right) \left(\frac{s}{s_0} \right)^{1 + \frac{kD_\perp}{6} + \alpha' t} \qquad (62)$$

with the extra s_0/s pre-factor accounting for the normalization of the spinors traveling on the exchanged world-sheet. This point was originally made in [14] but with different conclusions for the reggeon intercept. At large s, the pomeron exchange is dominant. The pomeron as a closed string can be viewed as 2 glued open strings or a pair of reggeons up to spin factors. As a result the reggeon slope is twice the pomeron slope while its intercept is also twice the pomeron intercept.

C. Entropy

The pomeron described here is a non-critical string in $D_\perp + 2 = 5$ dimensions in leading order in $1/\lambda$. We already commented how the temperature is formally introduced: the same can be done for the free energy $\mathbf{F} = -\ln \mathbf{K}_T/\beta_U$ and the entropy [1, 2]

$$\begin{aligned}\mathbf{S} = \quad & -D_\perp \sum_{n=1}^{\infty} \left(\ln\left(1 - e^{-\beta_k n}\right) + \frac{\beta_k n}{e^{\beta_k n} - 1} \right) \\ & + D_\perp \left(\frac{\beta_k}{12} - \frac{1}{2} \left(1 + \ln\left(\frac{\beta_k}{2\pi} \right) \right) \right) \end{aligned} \tag{63}$$

At large rapidity χ the entropy is dominated by the tachyon contribution

$$\mathbf{S} \approx \frac{D_\perp \beta_k}{12} \tag{64}$$

Since $\beta_k = 2\chi/k$ the entropy scales with the rapidity interval χ. In contrast, the energy $\mathbf{E} \approx \sigma\mathbf{b}$ with on average $\langle \mathbf{b}^2 \rangle \approx \mathbf{D}_k\chi$, scales with the root of the rapidity interval, and therefore is subleading for asymptotically large χ. This is a major difference between this regime and the explosive string that we will discuss below.

Large particle multiplicities in pp, pA and AA collisions based on (64) can be achieved through multiple pomeron exchanges [1, 2] as illustrated in Fig. 9. The multiple exchanges start to interact as they diffuse transversely. Their number density in transverse space is set by the squared stringy saturation scale [1, 2]. Although each exchange is penalized by $g_s^2 \approx 1/N_c^2$, it yields to a shadowing of the dipole-dipole cross section and saturation after an eikonalized resummation. The multiplicities are found to be consistent with the bulk multiplicities at current collider energies.

In this scenario, the exchanged strings are sub-critical with $T < T_H$. They may turn into an ideal fluid of string bits with very small viscosity [2]. The stringy matter is released sub-critical and non-explosive. It can transmute to a black-hole on a time scale of order $t \approx (\mathbf{b}/\chi)^3/(4l_s^2)$ after the percolation in transverse space [1].

D. Near-Hagedorn strings and the Nambu-Goto description

We recall that all the expressions discussed above such as (52) for instance, were derived using the scalar string or Polyakov action in the regime $\beta_H < \beta < \mathbf{b}$ dominated by the tachion mode $n = 0$

$$\mathbf{K}_T(\beta, \mathbf{b}; k) \approx \left(\frac{\beta}{4\pi^2 \mathbf{b}} \right)^{D_\perp/2} e^{-\sigma\beta\mathbf{b}\left(1 - \beta_H^2/2\beta^2\right)} \tag{65}$$

However, as the Unruh temperature becomes closer to the Hagedorn temperature or $\beta_U \to \beta_H$, string excitation is no longer small. Thus the use of the Polyakov action is no longer valid and β_H/β corrections need to be resummed. For $D_\perp = 3$ we have $\beta_H = 2\pi l_s$ so that $\beta_H \approx \beta_U$ requires $\mathbf{b} \approx \chi l_s/k$. This shortcoming is readily fixed by noting that (65) is just the large β asymptotic of the Nambu-Goto (NG) string action. The NG string is a conformal realization of the Polyakov string which is valid for smaller $\mathbf{b}$ and β. The re-summed result obtains a square root (which will play important role in what follows)

$$\mathbf{K}_T(\beta, \mathbf{b}; k) \approx \left(\frac{\beta}{4\pi^2 \mathbf{b}} \right)^{D_\perp/2} e^{-\sigma\beta\mathbf{b}\left(1 - \beta_H^2/\beta^2\right)^{1/2}} \tag{66}$$

In the NG realization of the pomeron the tachyonic contribution to the transverse propagator

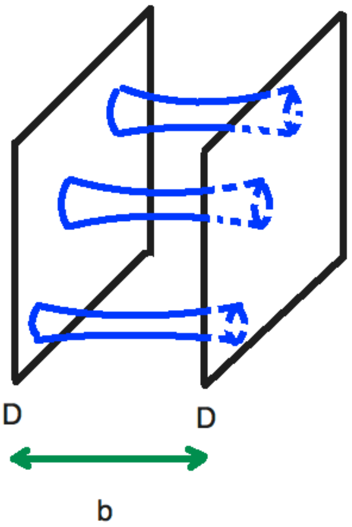

FIG. 9: Multi-pomeron contribution to dipole-dipole scattering near saturation with sub-critical string exchanges.

$\mathbf{K}_T$ is still dominated by the tachyon provided that the impact parameter is larger than the critical $\mathbf{b}_C = \pi l_s$. Clearly (66) reduces to (65) for $\beta_H/\beta \ll 1$.

The resummed expression (66) shows that the Unruh temperature causes the string tension to vanish at the Hagedorn point

$$\sigma\left(1-\beta_H^2/\beta^2\right)^{1/2} \to 0 \tag{67}$$

in agreement with the universal behavior observed for static thermal strings [31]. As we noted above, this occurs when the impact parameter $\mathbf{b} \approx \chi l_s$.

The scattering amplitude associated to the NG tachyon can be obtained by inserting (66) in (50). The result in the saddle point approximation reads

$$\mathcal{T}(s,t;1) \approx i g_s^2 \tag{68}$$
$$\left(\frac{s}{s_0}\right)^{\left(t/\sqrt{2}\right)\left(1-\frac{1}{4}(1+\sqrt{1-2/t})\right)\left(1+\sqrt{1-2/t}+1/t\right)^{1/2}}$$

with $t \equiv \alpha' t$ and $k=1$. (69) reduces to the pomeron amplitude (59) for $s \gg -t > 1/\alpha'$.

The cross section σ_{HM} for the production of near-critical strings or high multiplicity events follows from (50), by the optical theorem , with $q=0$ and $\mathbf{b} \approx \chi l_s$. Specifically, for dipole-dipole scattering with N-ality $k=1$, one finds

$$\begin{aligned}\sigma_{HM} \approx \quad & g_s^2 \left(\frac{\beta_H}{4\pi^2\chi l_s}\right)^{D_\perp/2} \\ & \times \left(\frac{\chi\beta_H}{\pi}\right)^2 \left(\frac{\Delta\beta}{\beta_H}\right) e^{-\chi\sqrt{\Delta\beta/2\beta_H}}\end{aligned} \tag{69}$$

with

$$\frac{\Delta\beta}{\beta_H} = \frac{T_H}{T} - 1 = \mathcal{O}\left(\frac{1}{N_c}\right) \tag{70}$$

The minimum bias cross section σ_{MB} has been estimated in [17] after an eikonal resummation of the subcritical strings,

$$\sigma_{MB} \approx \frac{\pi D_\perp \alpha'}{3}\chi^2 \tag{71}$$

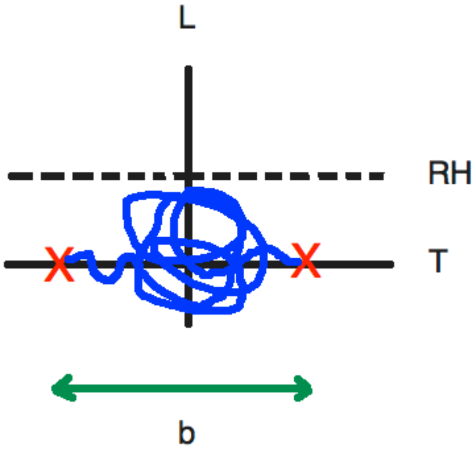

FIG. 10: The string ball: RH is the Rindler horizon along the longitudinal direction L, with the string streching along the transverse T direction with impact parameter **b**.

The ratio of the high multiplicity events to the minimum bias events can be estimated as

$$\frac{\sigma_{HM}}{\sigma_{MB}} \approx g_s^2 \frac{1}{\chi^{D_\perp/2}} \left(\frac{\Delta\beta}{\beta_H}\right) e^{-\chi\sqrt{\Delta\beta/2\beta_H}} \tag{72}$$

where we have dropped an overall number of order 1 and $D_\perp = 3$. For near critical strings we have (70) and $g_s \approx 1/N_c$. At LHC, $\chi \approx 10$ so that

$$\frac{\sigma_{HM}}{\sigma_{MB}} \approx 10^{-5} \tag{73}$$

This estimate is comparable to the probability of the high multiplicity trigger used by the CMS collaboration for events displaying the ridge in pp collisions at LHC.

E. The string ball as a black hole

We now show that the string at this point transmutes to a string ball (dual to a black-hole) with large energy and entropy. The near-Hagedorn pomeron has a horizon located along the *longitudinal* L-direction shown in Fig. 10. This is very different from the effective thermal AdS metric used in most of the thermal AdS/CFT studies of the sQGP because the horizon is *not* along the holographic z-direction. We note that the SZ model has a holographic z-coordinate in the T-transverse coordinates in Fig. 10, but with a confining wall at $z = z_0$, not a thermal horizon.

The pomeron propagator (66) behaves like a thermal ensemble with Unruh temperature $1/\beta_U$. We follow [1] and define the free energy or pressure $\mathbf{F} = -\ln\mathbf{K}_T/\beta_U$,

$$\mathbf{F}(\beta, \mathbf{b}) \approx k\sigma\, \mathbf{b} \left(1 - \frac{\beta_H^2}{\beta^2}\right)^{1/2} \tag{74}$$

At the near-Hagedorn regime with $\mathbf{b} \approx \chi l_s/k$ the pressure is small, but the energy and entropy are very large

$$\mathbf{E} = \partial_{\beta_U}(\beta_U k\mathbf{F}) \approx k\sigma\mathbf{b}\left(1 - \frac{\beta_H^2}{\beta^2}\right)^{-1/2} \tag{75}$$

$$\mathbf{S} = \beta_U^2 \partial_{\beta_U}\mathbf{F} \approx (\beta_H^2/\beta)k\sigma\mathbf{b}\left(1 - \frac{\beta_H^2}{\beta^2}\right)^{-1/2}$$

For $\beta \approx \beta_H$, the first law of thermodynamics for black-holes in Rindler coordinates as noted by Susskind [32], emerges with

$$\mathbf{S} \approx \beta_H \mathbf{E} = 2\pi\,(\mathbf{E} l_s) \tag{76}$$

and vanishingly small pressure (74). We note the Rindler temperature $T_R = 1/2\pi$ and therefore the Rindler energy $\mathbf{E}_R = \mathbf{E} l_s$. The emergence of a Rindler temperature is expected since the stringy pomeron exchange is characterized by a line element [1]

$$ds^2 \approx -a^2\,\rho^2 dt^2 + d\rho^2 + ds_\perp^2 \tag{77}$$

with a Rindler acceleration $a = \chi/\mathbf{b}$. At this regime the acceleration is $a = k/l_s$. On the streched horizon at $\rho = l_s/k$ in (77), the warping of time is 1 since $t/t_\rho = (b/\chi)/\rho \to l_s/k\rho$. A cartoon of the string ball as a black-hole is shown in Fig. 10.

The transverse area of the black-hole is the area of the diffusing string in rapidity

$$A_{BH} = 2\pi^2 \left(\sqrt{\chi/k}\, l_s\right)^3 \tag{78}$$

in transverse $D_\perp = 3$ provided that the diffusion length in the z-direction is within the confining wall. As a result, we have the Bekenstein-Hawking type relation

$$\frac{\mathbf{S}_{BH}}{A_{BH}} \equiv \frac{1}{4G_5} \tag{79}$$

with an effective Newton constant

$$G_5 = \pi^2\left((\chi/k^3)(1 - \beta_H^2/\beta^2)\right)^{1/2}\, l_s^3 \tag{80}$$

For a fundamental string, the Planck and string constants tie with G_5 through $G_5 = l_P^3 = g_s^2 l_s^3$, with in general $g_s^2 \approx 1/N_c^2$.

The transmutation of the fundamental string to a black-hole at the string scale was foreseen by Susskind and others in the context of string-based gravity [32, 33]. Indeed, through an isentropic variation of the string coupling $g_s \to 0$ as a trick, it was argued that the Bekenstein-Hawking formulae emerges from a statiscal counting of quantum string states. In hadronic collisions at large rapidity χ, the effective relation (80) shows that this transmutation can be achieved in a twofold way: 1/ $\beta/\beta_H \to 1$ (Hagedorn limit); 2/ $k/\chi \to \infty$ (large N-ality or N_c limit). The Hagedorn regime can be achieved through fluctuations with high multiplicity events at current collider energies in pp, pA and AA experiments as we suggested above.

Empirical estimates based on DIS data analysis suggests $z_0 \approx 2/\text{GeV}$ [1], so that the diffusion length is within the confining wall for $\sqrt{\chi/k} l_s < z_0$ or $\chi < 16$ for $k = 1$. For $\chi > 16$ the diffusion length is outside the confining wall and the transverse area (78) is now changed to

$$A_{BH} \approx 2\pi^2 z_0 \left(\sqrt{\chi/k}\, l_s\right)^2 \tag{81}$$

with the corresponding changes in the effective Newton constant estimate

$$G_5 = (\pi^2/k)\left(1 - \beta_H^2/\beta^2\right)^{1/2}\,(z_0 l_s^2) \tag{82}$$

F. String on the Rindler horizon

At the near-Hagedorn regime the pomeron string carries large energy and entropy but vanishingly smal pressure. To assess the transverse viscosity of this string without recourse to a full Nambu-Goto analysis, we make the key observation that in near Hagedorn regime the exponents in (63) transmute to

$$\beta_k n \to \beta_R\, n \tag{83}$$

with n the Rindler frequency of the harmonic oscillator. At large $1/\beta_k$ or large Rindler temperature $1/\beta_R$, the string energy and entropy are dominated by the high modes in (63). We have explicitly checked that the tachyon thermodynamics (74) and (76) follow from the large n excitation spectrum of the NG string by using the modular transformation and the saddle point approximation, as we detail in Appendix B.

At the Hagedorn limit, a long and space filling string, with $D_\perp$ dimensions, is a very efficient way to carry large entropy. The analogy between a string ball and black hole thermodynamics shows that in fact it carries the largest entropy density possible! With this in mind and for simplicity, consider a Polyakov string made of $D_\perp$ harmonic oscillators immersed in a heat bath with finite but large Rindler temperature $1/\beta_R$. The energy of the string is dominated by the high frequency modes,

$$\mathbf{E}_R \approx D_\perp \sum_{n=1}^{\infty} \frac{n}{e^{\beta_R n} - 1} \tag{84}$$

For large $1/\beta_R$ it is black-body

$$\mathbf{E}_R \approx \frac{\pi^2}{2\beta_R^2}\frac{D_\perp}{3} \tag{85}$$

Through the first law of thermodynamics (76) we can enforce the zero pressure condition on this highly excited string, with

$$\mathbf{S} \equiv \mathbf{S}_R \approx \beta_R \mathbf{E}_R = \frac{\pi^2}{2\beta_R}\frac{D_\perp}{3} \tag{86}$$

G. Viscosity at the Rindler horizon

Viscosity can be defined via certain limits of the correlators of the stress tensor, known as the Kubo formula. Thus one does not need hydrodynamics to calculate it, just the stress tensor. To assess the primordial viscosity, we follow [2] and write the needed expression on the streched horizon for the excited string

$$\eta_R = \lim_{\omega_R \to 0} \frac{A_R}{2\omega_R} \int_0^\infty d\tau e^{i\omega_R \tau} \mathbf{R}_{23,23}(\tau) \tag{87}$$

with A_R the area of the black-hole and τ a dimensionless Rindler time. The retarded commutator of the normal ordered transverse stress tensor for the Polyakov string on the Rindler horizon reads

$$\mathbf{R}_{23,23}(\tau) = \left\langle \left[T_\perp^{23}(\tau), T_\perp^{23}(0)\right] \right\rangle \tag{88}$$

with

$$T_\perp^{23}(\tau) = \frac{1}{2A_R} \sum_{n\neq 0} :a_n^2 a_n^3: \, e^{-2in\tau} \tag{89}$$

and the canonical rules $\left[a_m^i, a_n^j\right] = m\delta_{m+n,0}\delta^{ij}$. The averaging in (88) is carried using the black-body spectrum as in (84). The result is

$$\eta_R = \lim_{\omega_R \to 0} \frac{A_R}{2\omega_R} \frac{\pi}{2A_R^2} \frac{(\omega_R/2)^2}{e^{\beta_R \omega_R/2} - 1} = \frac{1}{A_R}\frac{\pi}{8\beta_R} \tag{90}$$

We note the occurence of the Bekenstein-Hawking or Rindler temperature $\beta_{BH} = \beta_R$ in the thermal factor.

Combining (86) for the entropy to (90) yields the viscosity on the streched horizon

$$\frac{\eta_R}{\mathbf{S_R}/A_R} = \frac{1}{4\pi}\left(\frac{3}{D_\perp}\right) \equiv \frac{1}{4\pi} \tag{91}$$

which, for $D_\perp = 3$, is precisely the celebrated universal value from AdS/CFT. The result (91) is remarkable as it follows solely from a string moving at large "time" χ in non-critical dimensions but near its Rindler horizon, not in transverse coordinate z. It emerges naturally in the near-Hagedorn regime.

The result (91) for the critical pomeron as a close string exchange on the streched horizon for large $1/\beta_R$ is to be contrasted to the same viscosity ratio but for the low-T pomeron as a close string exchange far from the horizon for small $1/\beta_k$ [2]

$$\frac{\eta_\perp}{\mathbf{S}/A_\perp} = \frac{1}{2}\frac{1}{4\pi}\left(\frac{2\pi}{\beta_k}\right)^2\left(\frac{3}{D_\perp}\right) \tag{92}$$

The ratio is small at large rapidity. (92) reduces to (91) for $\beta_k \to \beta_R$ up to a factor of 1/2, showing the non-commutativity of the two limits. Indeed, for small $1/\beta_k$ the non-critical pomeron is described by the Polyakov action whereby the zero pressure condition (emblematic of a near-Hagedorn or black-hole in Rindler coordinates) does not hold.

In light of (40) above it is amusing to note that the stringy relation (90) yields on the Rindler horizon an effective viscosity for finite frequency but zero momentum

$$\eta_R(\omega_R) = \frac{\pi}{16A_R}\frac{\omega_R}{e^{\omega_R/2T_R}-1} \tag{93}$$

(93) thermally suppresses the large frequency modes ω_R. The on-set of the black-hole is followed by black-body or Hawking radiation of string bits of frequency $\omega_R/2$ as is explicit in (93) and stressed further below. In particular, for finite wavenumber k_R in Rindler units, the suppression is physically expected to follow from the substitution

$$\omega_R \to \sqrt{\omega_R^2 + k_R^2} \tag{94}$$

and therefore exponential as well. The effective viscosity $\eta_R(\omega_R, k_R)$ at higher gradients – larger k_R– would indeed imply a smaller effective viscosity in pp than in AA, as we discussed earlier in the LS re-summation and also from phenomenology.

Concluding this discussion of the viscosity let us point out that while we can use the Kubo formula for any setting in which the stress tensor is defined, the viscosity itself is of hardly any use outside the hydrodynamical setting. And alas, both for the cool subcritical strings and the near-Hagedorn critical strings we so far considered, there is no hydrodynamics involved. However, this is going to change as we now discuss.

H. Very high multiplicity and transition to sQGP

The typical (minimal bias) dipole-dipole – and thus pp, pA and AA collisions – involve the exchange of pomerons and reggeons in the subcritical regime with low entropy/multiplicity and low $T < T_H$. At very large $\sqrt{s}$ the cross section and the string impact parameter $\mathbf{b}$ grow, and eventually the possibility of observing string fluctuations in the near-Hagedorn regime becomes increasingly probable.

Furthermore, as the entropy density grows further, the string eventually fills the space and its *repulsive* self-interaction becomes important. In thermodynamics this is seen as the end of the Hagedorn regime (the high end of the mixed phase) from which the system goes into a deconfined phase. We now suggest that an individual string ball reaching such an entropy density (corresponding to the point B in Fig.2) does the same. Its entropy density S/T^3 stops growing. From (79) the onset is expected when the (Bekenstein-Hawking) entropy becomes as large as that of the gluons, which coresponds to

$$\frac{\mathbf{S}_{BH}}{A_{BH}} \equiv \frac{1}{4G_5} \approx \frac{N_c^2}{\beta_H^3} \tag{95}$$

Note that at large N-ality $k \approx 1/N_c$, so that the transition takes place very close to the Hagedorn temperature $\beta/\beta_H - 1 = \mathcal{O}(1/N_c)$. As soon as the string entropy gets so high, the pressure is no longer small, eventually reaching $\epsilon/3$ as for a gluonic gas, so an explosion follows.

We suggest that these explosive events are triggered in the current LHC collider in pp and pA events. The black-hole explosion is signaled by a large radial and elliptic flows in the large multiplicity events.

Let us now estimate the critical multiplicity above which such explosion should happen. The multiplicity $\mathbf{N}$ associated with the explosion of the black-hole is readily estimated from the entropy near the Hagedorn transition subject to the condition (95). Indeed,

$$\mathbf{N} \approx 7.5\,\mathbf{S} \approx \sigma\beta_H\mathbf{b}\left(1-\beta_H^2/\beta^2\right)^{-1/2} \tag{96}$$

where the conversion factor of 7.5 is borrowed from the entropy-to-hadron density relation at freeze out. Substituting $\beta_H/\beta - 1 \approx 1/N_c$ from (95), we find the critical charge particle multiplicity to be

$$\mathbf{N} \approx 7.5\,\mathbf{S} \approx 7.5\,\chi/2 \approx 45 \tag{97}$$

after using that $\mathbf{b} \approx \chi\, l_s$ and $\chi \approx 12$ at the LHC. The estimate (97) can be compared with the measured threshold multiplicity of $N > 50$ for events with the ridge, according to the CMS collaboration [8]. However, we note that the actual acceptance of the CMS detector in rapidity and more importantly in p_t, will increase the latter number by about a factor of 2 or so. The freeze out conditions are probably also different in pp and pA from AA (from which the 7.5 factor is taken). Only further studies of spectra in "explosive" events will make a comparison quantitative.

I. Hawking radiation

The typical pp,pA collisions create strings which decay via Schwinger pair-production mechanism, which is described by the Lund model, PITHIA etc. The proposed black-hole-like description –dual to a string ball – we ascribed to high-multiplicity events leads naturally to a different particle emission mechanism, namely via the Hawking radiation. This emission is fully thermal from the prompt emission, and not delayed as in string breaking mechanism. Let us note that our approach is similar in spirit but different in details to the Unruh-Hawking effect discussed in [34]. In particular, in this paper the Unruh temperature is related to acceleration created by a string, not a collective "effective gravity" of the string ball as a whole, as in our model.

The power spectrum or Hawking emission per unit time from a black-hole is generic. For our rapidly moving string it involves a black-hole in $1+4$ dimensions with the extra dimension accounting for changes in the dipole scales. In $D_\perp + 2$ dimensions it reads

$$d^{D_\perp+1}\mathbf{P} = \tag{98}$$
$$\sum_s \sigma_s(\omega) \frac{\omega}{e^{\omega/T_{BH}} + (-1)^{2s+1}} \frac{d^{D_\perp+1}k}{(2\pi)^{D_\perp+1}}$$

We have only kept the dominant S-wave contributions. Here $T_{BH} = T_R = 1/(2\pi l_s)$. The sum runs over the spin s of the emitted particle with $\sigma_s(\omega)$ the S-wave absorption cross section or grey-body factor of a spin-s on a black-hole. For $\omega l_s \ll 1$

$$\sigma_s(\omega) \approx \kappa_s\, A_{BH} \equiv 4\kappa_s l_P^{D_\perp+1}\,\mathbf{S} \tag{99}$$

with A_{BH} the area of the black-hole. The last identity follows from the Bekenstein-Hawking type relation and shows that the power spectrum is extensive with the entropy. For scalars $\kappa_s = 1$ [35]. As the Hawking emission through (99) unfolds, the mass and radius of the black-hole decreases, causing the Hawking temperature T_{BH} to increase. The emission process is inherently a non-equilibrium one. Here and for simplicity we assume it to be quasi-adiabatic with (99) adjusting to the change in T_{BH}.

For massless particles $\omega = |k|$ in (99). The luminosity defined as $\mathbf{L}(\omega) = d\mathbf{P}/d\omega$ for $D_\perp = 3$ is

$$\mathbf{L}(\omega) = \frac{A_{BH}}{8\pi^2} \sum_s \kappa_s \frac{\omega^4}{e^{\omega/T_{BH}} + (-1)^{2s+1}} \tag{100}$$

It is a black-body spectrum from a 5-dimensional space where the black-hole originated from.

As many of these black-holes are expected to be released in AA collisions they are the seeds of the primordial matter viewed as a collection of these tiny black holes. Primordial Hawking emission of partonic constituents as well as electromagnetic radiation is what current heavy ion colliders are probing. We recall that for $\chi < 16$ we have $A_{BH} \approx \chi^{3/2}$ while for $\chi > 16$ we have $A_{BH} \approx \chi$ because of confinement in the holographic or conformal direction of the string. Therefore, we estimate the tresholds $\mathbf{N}_T(\chi)$ for the large multiplicity events with explosive hydrodynamical flow to scale with beam rapidity as

$$\frac{\mathbf{N}_T(\chi_1)}{\mathbf{N}_T(\chi_2)} = \left(\frac{\chi_1}{\chi_2}\right)^{3/2} \tag{101}$$

for $\chi_{1,2} < 16$ and 1 for $\chi_{1,2} > 16$, irrespective of whether it is pp, pA and AA collisions.

V. SUMMARY AND DISCUSSION

High multiplicity pp and pA collisions are very interesting systems which are supposed to display a transtion from a "micro" to "macro" dynamical regime. In this paper we tried to explain how this transition works using the language of both macroscopic and microscopic theory.

We started in the "macro-to-micro" limit, using the hydrodynamical framework. As we emphasized in the Introduction, the applicability of hydrodynamics to high energy collisions rests on *two* small parameters: (i) the micro-to-macro ratio $1/TR$, (ii) the viscosity-to-entropy ratio η/s. For central AA collisions, both are small or of order $\mathcal{O}(1/10)$. For high multiplicity pA and pp collisions, the first parameter is no longer small $1/TR = \mathcal{O}(1)$, prompting us to ask which hydrodynamical predictions are preserved by the smallness of only the second parameter η/s.

After solving the hydrodynamical equations we found that the *radial* (axially symmetric) flow is little modified by viscosity and is in fact enhanced by higher transverse gradients. Thus our main prediction is an *enhanced radial flow.* Its signatures are well known [4] with specifically a change in the observed p_t spectra on the particle mass, or growing proton-to-pion-ratio with p_t. The magnitude of the effect should be even larger than in AA collisions, see (17) for specific values of the maximal transverse velocity calculated in the Gubser flow.

However, higher harmonics are more penalized by viscous corrections. We used the generic high-harmonics expression from [22] and obtained explicit solutions for Gubser flow for $m = 2, 3, 4$ as shown in Fig.6. We have found a small $v_3/v_2 \approx 1/3$ ratio for pA in agreement with the reported ALICE data (to be compared to the value above 1 in central AA). The value of v_2 itself is also suppressed by viscosity, and the relative suppression we have found between the pp and pA collisions agree reasonably with the CMS data.

Then we discussed the problem in the opposite "micro-to-macro" limit, in the framework of a holographic QCD string pomeron. We have reviewed the general arguments behind the SZ pomeron as an exchange of a non-critical string in curved AdS$_5$ with confinement. For long strings with $\beta > \beta_H$, the pomeron follows from the scalar Polyakov action for the slightly excited string oscillators. The Luscher term generates the intercept of the pomeron (59), which for $D_\perp = 3$ and, with a finite $1/\lambda$ correction, yields its phenomenological value of 0.08.

The fluctuations in "hotter" strings show that their effective Unruh temperature may become close to the Hagedorn temperature of the gluodynamics strings. Because of the Polyakov-Susskind phenomenon, string excitations are no longer small. The string shape is better described by a Nambu-Goto string instead of a scalar or Polyakov string. For such a large amplitude of excitation a *"string ball"* forms, with a large energy and entropy, yet a small pressure. The ensuing dynamics closely resembles what takes place in equilibrium thermodynamics in the mixed phase of pure gauge theory. We have shown that it is dual to a miniature black-hole with a Rindler horizon along the longitudinal direction of the collision. This black-hole is 5 dimensional, with 3 transverse coordinates, 2 spatial ones and 1 conformal z describing the scale evolution. The black-hole radius and area are set by the Gribov diffusion length, which grows with the collision energy $\chi = \ln(s/s_0)$ as $\chi^{1/2}$, and $\chi^{3/2}$ for $\chi < 16$, respectively. For $\chi > 16$ the area growth is reduced to χ because of confinement along the holographic or conformal direction of the string.

Using the Kubo formula for string excitations, we found that on the stretched or Rindler horizon the shear viscosity to entropy ratio is precisely $1/4\pi$, for $D_\perp = 3$. It is the same as for AdS/CFT black hole, in spite of the fact that these two black holes are very different. Ours is dynamical with a horizon normal to the longitudinal coordinate, while the AdS/CFT one is static, with a horizon normal to the transverse holographic z-direction.

We have argued that when the Unruh temperature narrows even closer on the Hagedorn temperature, with $T/T_H - 1 = \mathcal{O}(1/N_c)$, the Bekenstein-Hawking relation for the stringy black-hole becomes partonic and the ball of strings turns into a sQGP fireball. As a result, transition to deconfined phase unleashes a large pressure with $p \approx \epsilon/3$ and the stringy black-hole explodes hydrodynamically, following the general scaling of viscous hydrodynamics in small volumes, as we discussed above. Our estimates put the trigger for such high multiplicity events at LHC at 10^{-5} which is comparable to the currently used trigger of 10^{-6} for pp collisions used by the LHC collaboration.

Our estimates show that the treshold multiplicity for the explosive pomerons is about $\mathbf{N} \approx 45$ for pp collisions with a rapidity interval of $\chi \approx 12$. After outlying the suggested theoretical scenario, let us focus on its possible experimental tests. The most obvious of these tests consists in further investigating whether the "ridge" is indeed a collective phenomenon, rather than a correlation of few particles. It is by now well known how to carry this: one should compare the elliptic flow parameters extracted from 2,4,6 particles. Collective phenomena induce approximately factorizable multiparticle distributions, while dynamical correlations (like mini-jets) disappear in many-body correlators. Another obvious direction is to look for the "ridge" and related phenomena at RHIC energies.

Our main proposal is to search for the radial flow, using spectra of identified particles, which ALICE, PHENIX and STAR can do in their pA sample, or perhaps even in their pp samples. If successful, one may use hydrodynamics backward in time and derive the fireball sizes R for the pp and pA systems at different multiplicity and collision energy, to be compared with our "ball of string" scenario. Perhaps one can even create string-based event generators and predict the elliptic fluctuations of such a ball and compare it to the v_2 observed as the (now famous) "double ridge".

Finally, we now discuss some important differences between our string based scenario and other models, and emphasize the differences in their microscopic dynamics. A rather comprehensive description of the LHC pp and pA data has been done recently by Dusling and Venugopalan [36] using 1- and 2-pomeron exchanges made of perturbative pomerons of the BFKL type. For typical collisions our string-based pomeron and their approach would perhaps agree, although our pomerons follow from strong coupling and large N_c QCD.

In contrast, the physics of small-probability and large-amplitude fluctuations we have discussed in this work is fundamentally different. Weak coupling logic leads to *saturation* and "glasma", an ensemble of classical gluonic fields with Gaussian fluctuations. The string approach we use is remarkably different: while the gluonic fields are also strong, they are confined into thin flux tubes, which have a very unusual dynamics and thermodynamics. At certain near-critical conditions (realized also for equilibrium gluodynamics as a "mixed phase") strings get "soft" and produce large energy/entropy clusters we called "string balls". Such clustering to very high density is in a way opposite to saturation. String clustering instead of saturation is natural in effective gravity. Indeed, the thermodynamics of the string balls can indeed mimic that of the black holes. Note that these ideas, while foreseen in general terms in [34], became only quantitative with the AdS/CFT correspondence and other studies of gauge-string-gravity dualities in the last decade. Its dynamical details still need a lot of work to be understood. One key feature of this approach is the completely different view on thermalization. Instead of rescattering of incoming gluons, as done in weak coupling, it is instead a quasi-instantaneous [1] Hawking radiation of new quarks and gluons induced by the effective "gravity" of the cluster near its horizon.

Speaking about experimental tests of those divergent scenarios, let us first note the (somewhat forgotten) issue of *quark chemical equilibration.* We know from the structure functions that at high energies that the excited system produced should be mostly gluonic, with a small quark admixture. Perturbative logics lead to the so called "hot glue" scenario [37] in which quarks appear several fm/c later. Recent glasma models lead to similar conclusions. In contrast, the prompt black-hole formation and its ensuing Hawking type radiation should include both quarks and gluons promptly. This point is supported indirectly by hydrodynamical applications: they work well, assuming prompt quark equilibration.

The way to check this is through the production of photons and dileptons. The effective gravity and black holes are for strong interactions only, so photons and leptons are only produced through a secondary radiation by black-body quarks. At RHIC the best place to tell the "hot glue" scenario from the full QGP one, is to look at intermediate mass dileptons, with a mass range of $1-3$ GeV. Unfortunately, the contamination of these leptons by charm decays remains an unresolved issue, which requires high-resolution vertex detectors.

Another suggestion is to study the statistics of fluctuations. If pA data are to be interpreted as we suggest, it means that with the order of a few percent probability a "string ball" cluster is produced (and explodes into the double ridge). If so, in AA collisions the probability of this phenomenon should be $O(1)$, as we have hundreds of nucleons going through the near-center of another nucleus. While being only a small part of the fireball, the stringy cluster is a significant local perturbation of the initial conditions, resulting in sound waves and correlations of flow harmonics. This phenomenon obviously is *not* included in the standard Glauber theory of fluctuations, and perhaps can be revealed by flow harmonics correlations, induced by a localized source [24].

Acknowledgements. We would like to thank our students Alex Stoffers and Pilar Staig for their help in developing many of the ideas presently discussed. We also thank Gokce Basar, Dima Kharzeev and Derek Teaney for discussions. This work was supported by the U.S. Department of Energy under Contract No. DE-FG-88ER40388.

Appendix A: The first harmonics and the recoil mass

The first harmonics of the correlation function has a special role since it is dominated not by flow per se but by the *momentum conservation.* It is usually considered to be just an uninteresting observable. For example no discussion of this point is given in Refs. [7–9].

Borghini and collaborators [30] had calculated its magnitude assuming that all the transverse momentum of the trigger is absorbed by *all* secondaries equally. This implies that the fireball as a whole moves with certain small velocity $\vec{P}/M$ where M is its total mass. The conditional probability in the 2-particle distribution is

$$f(\vec{p_2}|p_1) = f_0(\vec{p_2})\left(1 - \frac{2p_1 p_{2,x}}{N\left\langle p_t^2\right\rangle(1+\bar{v}_2)}\right) \tag{A1}$$

where the trigger , by definition, moves in the x direction,

$$\bar{v}_2 = \frac{\left\langle p_x^2 - p_y^2\right\rangle}{\left\langle p_x^2 + p_y^2\right\rangle} \tag{A2}$$

and the correction containing it appears here because in the denominator one has $\left\langle p_x^2\right\rangle$ not the whole p_t.

First, let us argue that an assumption that all particles in the fireball can share the trigger momentum cannot possibly be true, since it contradicts hydrodynamical casuality. Indeed, in a hydrodynamical regime a perturbations cannot propagate faster than the speed of sound. Thus N in the formula above should be no larger than the number of particles *inside the sound horizon*, from a trigger emission event. We then predict that in the magnitude of the v_1 one should use $N_{recoil}/N_{tot} < 1$.

One can estimate it as

$$\frac{N_{recoil}}{N_{tot}} = \frac{H_s^2}{R^2}\frac{2c_s\tau_f}{\Delta Y} \approx 1/3 \tag{A3}$$

where the first factor is the transverse and the second longitudinal, $\Delta Y \approx 10$ is the total rapidity interval between the beams.

Let us now have a look at the experimental data. The fit for RHIC PHOBOS data gives

$$V_{1\Delta} \approx -1.510^{-3} \tag{A4}$$

Substituting $\bar{v}_2 \approx 0.2$ and the mean square transvserse momenta, plus integrating it over momenta p_2 one gets the number of particles which are getting the "recoil"

$$N_{recoil} = \frac{p_1 < p_t >}{V_{1\Delta}\left\langle p_t^2\right\rangle(1+\bar{v}_2)} \approx 500 \tag{A5}$$

Indeed, that it is significantly smaller than the total multiplicity of the events in the corresponding centrality class 10-20% of RHIC AuAu collisions $N_{tot} \approx 3000$.

Our second proposal is to look not at the average but the distribution over the value $P(v_1)$ and interpret it in terms of the "recoil mass distribution". It is expected to be very different in different models, and perhaps such data would have some discriminative power.

For pA and pp collisions: systems much smaller than the central AA should have smaller recoil mass and larger recoil velocity, thus larger first harmonics. While extracting it from back-to-back jet component is not so easy, we urge experimentalists to measure the first harmonics as it contains important information.

Appendix B: Large n spectrum of string excitations

It is interesting to note that the tachyon thermodynamics can be alternatively derived by using the modular transform of the transverse string propagator, (nearly) exchanging $b \leftrightarrow \beta$ and exchanging the close and open string descriptions. Indeed, the modular transform of (52) can be cast as

$$\mathbf{K}_T(\beta, \mathbf{b}; k) \approx \sum_{n=0}^{\infty} d(n)\, e^{-\sigma\beta\mathbf{b}\left(1-\mathbf{b_c}^2/\mathbf{b}^2+2\pi n/\sigma\mathbf{b}^2\right)^{1/2}} \tag{B1}$$

with $\mathbf{b_c} = ((\pi D_\perp)(12\sigma))^{1/2} \equiv \pi l_s$ and the density of states (55). The NG form has been subsumed. (B1) is seen to diverge for $\beta \leq \beta_H$. The divergence is controlled by a large n saddle point,

$$n_S \approx \frac{\sigma\mathbf{b}^2}{2\pi}\frac{1}{(\beta/\beta_H)^2-1} \gg 1 \tag{B2}$$

for which (B1) is to exponential accuracy

$$\mathbf{K}_T(\beta, \mathbf{b}; k) \approx e^{-\sigma\mathbf{b}\sqrt{\beta^2-\beta_H^2}} \tag{B3}$$

in agreement with the tachyon result above.

The string energy at the large n saddle point (B2) is

$$\mathbf{E} \approx \sigma\mathbf{b}\sqrt{\frac{2\pi n_S}{\sigma\mathbf{b}^2}} = \frac{\sigma\mathbf{b}}{\sqrt{\beta^2/\beta_H^2-1}} \tag{B4}$$

and the corresponding entropy is

$$\mathbf{S} \equiv \ln d(n_S) = 2\pi\sqrt{\frac{D_\perp n_S}{6}} - \frac{D_\perp}{4}\ln n_S \tag{B5}$$

which is seen to satisfy the zero pressure condition $\mathbf{S} \approx \beta_H\mathbf{E}$ in leading order. They are the tachyonic energy and entropy in the Hagedorn limit discussed above. This is expected since the modular transform allows us to cross from the $\beta < \mathbf{b}$ regime of long and close strings, to the $\beta > \mathbf{b}$ of short and open strings. The two descriptions match at the border $\mathbf{b} \approx \beta$.

---

[1] A. Stoffers and I. Zahed, arXiv:1211.3077 [nucl-th].

[2] I. Zahed, arXiv:1211.6421 [hep-ph].

[3] E. V. Shuryak, Phys. Lett. B **78**, 150 (1978) [Sov. J. Nucl. Phys. **28**, 408 (1978)] [Yad. Fiz. **28**, 796 (1978)].

[4] E. V. Shuryak and O. V. Zhirov, Phys. Lett. B **89**, 253 (1979).

[5] T. C. Brooks *et al.* [MiniMax Collaboration], Phys. Rev. D **61**, 032003 (2000) [arXiv:hep-ex/9906026].

[6] Observation of Long-Range, Near-Side Angular Correlations in Proton-Proton Collisions at the LHC, The CMS Collaboration, submitted to Journal of High Energy Physics, presented at CERN seminar Sept.21,2010.

[7] S. Chatrchyan *et al.* [CMS Collaboration], [arXiv:1210.5482 [nucl-ex]].

[8] B. Abelev *et al.* [ALICE Collaboration], arXiv:1212.2001 [nucl-ex].

[9] G. Aad *et al.* [ATLAS Collaboration], arXiv:1212.5198 [hep-ex].

[10] E. Shuryak, arXiv:1009.4635 [hep-ph].

[11] P. Bozek, Phys. Rev. C **85**, 014911 (2012) [arXiv:1112.0915 [hep-ph]].

[12] E. A. Kuraev, L. N. Lipatov and V. S. Fadin, Sov. Phys. JETP **45**, 199 (1978) Ya. Ya. Balitsky and L. N. Lipatov, Sov. J. Nucl. Phys. **28**, 22 (1978)

[13] M. Rho, S. -J. Sin, I. Zahed, Phys. Lett. **B466**,

199-205 (1999). [hep-th/9907126].

[14] R. A. Janik and R. B. Peschanski, Nucl. Phys. B **565**, 193 (2000) [hep-th/9907177]; Nucl. Phys. **B625**, 279-294 (2002). [hep-th/0110024]; Nucl. Phys. **B586**, 163-182 (2000). [hep-th/0003059]; R. A. Janik, Phys. Lett. B **500**, 118 (2001) [hep-th/0010069].

[15] J. Polchinski and M. J. Strassler, JHEP **0305**, 012 (2003) [hep-th/0209211]; R. C. Brower, J. Polchinski, M. J. Strassler and C. I. Tan, JHEP **0712**, 005 (2007) [hep-th/0603115]; R. C. Brower, M. J. Strassler and C. -ITan, JHEP **0903**, 092 (2009) [arXiv:0710.4378 [hep-th]].

[16] L. Cornalba, M. S. Costa and J. Penedones, Phys. Rev. Lett. **105**, 072003 (2010) [arXiv:1001.1157 [hep-ph]]; L. Cornalba, M. S. Costa, J. Penedones and P. Vieira, JHEP **0612**, 023 (2006) [hep-th/0607083].

[17] G. Basar, D. E. Kharzeev, H. -U. Yee and I. Zahed, arXiv:1202.0831 [hep-th].

[18] M. Teper, Acta Phys. Polon. B **40**, 3249 (2009) [arXiv:0912.3339 [hep-lat]].

[19] S. S. Gubser, Phys. Rev. D **82**, 085027 (2010) [arXiv:1006.0006 [hep-th]].

[20] S. S. Gubser and A. Yarom, Nucl. Phys. B **846**, 469 (2011) [arXiv:1012.1314 [hep-th]].

[21] M. Lublinsky and E. Shuryak, Phys. Rev. D **80**, 065026 (2009) [arXiv:0905.4069 [hep-ph]].

[22] P. Staig and E. Shuryak, Phys. Rev. C **84**, 034908 (2011) [arXiv:1008.3139 [nucl-th]].

[23] R. A. Lacey, Y. Gu, X. Gong, D. Reynolds, N. N. Ajitanand, J. M. Alexander, A. Mwai and A. Taranenko, arXiv:1301.0165 [nucl-ex].

[24] P. Staig and E. Shuryak, Phys. Rev. C **84**, 044912 (2011) [arXiv:1105.0676 [nucl-th]].

[25] G. Policastro, D. T. Son and A. O. Starinets, Phys. Rev. Lett. **87**, 081601 (2001) [hep-th/0104066].

[26] S. Bhattacharyya, V. Hubeny, S. Minwalla and M. Rangamani, JHEP **0802**, 045 (2008) [arXiv:0712.2456 [hep-th]].

[27] E. Shuryak, Phys. Rev. C **86**, 024907 (2012) [arXiv:1203.6614 [hep-ph]].

[28] M. P. Heller, R. A. Janik and P. Witaszczyk, Phys. Rev. Lett. **108**, 201602 (2012) [arXiv:1103.3452 [hep-th]].

[29] D. Teaney, Phys. Rev. C **68**, 034913 (2003) [nucl-th/0301099].

[30] N. Borghini, PoS LHC **07**, 013 (2007) [arXiv:0707.0436 [nucl-th]].

[31] R. D. Pisarski and O. Alvarez, Phys. Rev. D **26**, 3735 (1982).

[32] L. Susskind, In *Teitelboim, C. (ed.): The black hole* 118-131 [hep-th/9309145]; L. Susskind, Phys. Rev. D **49**, 6606 (1994) [hep-th/9308139].

[33] A. Strominger and C. Vafa, Phys. Lett. B **379**, 99 (1996) [hep-th/9601029]; G. T. Horowitz and J. Polchinski, Phys. Rev. D **55** (1997) 6189 [hep-th/9612146]; R. R. Khuri, Nucl. Phys. B **588**, 253 (2000) [hep-th/0006063].

[34] D. Kharzeev, Eur. Phys. J. A **29**, 83 (2006); P. Castorina, D. Kharzeev and H. Satz, Eur. Phys. J. C **52**, 187 (2007) [arXiv:0704.1426 [hep-ph]].

[35] S. R. Das, G. W. Gibbons and S. D. Mathur, Phys. Rev. Lett. **78**, 417 (1997) [hep-th/9609052].

[36] K. Dusling and R. Venugopalan, arXiv:1211.3701 [hep-ph]; arXiv:1210.3890 [hep-ph]; Phys. Rev. Lett. **108**, 262001 (2012) [arXiv:1201.2658 [hep-ph]].

[37] E. V. Shuryak and L. Xiong, Phys. Rev. Lett. **70**, 2241 (1993) [hep-ph/9301218].